TEN MICRON POLARIMETRY OF COMPACT INFRARED SOURCES

by

Richard Warren Capps

A Dissertation Submitted to the Faculty of the

DEPARTMENT OF ASTRONOMY

In Partial Fulfillment of the Requirements
For the Degree of

DOCTOR OF PHILOSOPHY

In the Graduate College

THE UNIVERSITY OF ARIZONA

1 9 7 6

THE UNIVERSITY OF ARIZONA

GRADUATE COLLEGE

I hereby recommend that this dissertation prepared under my direction by Richard Warren Capps

entitled Ten Micron Polarimetry of Compact Infrared Sources

be accepted as fulfilling the dissertation requirement for the degree of Doctor of Philosophy

Dissertation Director — Date: 9th Nov 1976

As members of the Final Examination Committee, we certify that we have read this dissertation and agree that it may be presented for final defense.

	9th Nov 1976
	9th Nov 1976
	15 Nov

Final approval and acceptance of this dissertation is contingent on the candidate's adequate performance and defense thereof at the final oral examination.

STATEMENT BY AUTHOR

This dissertation has been submitted in partial fulfillment of requirements for an advanced degree at The University of Arizona and is deposited in the University Library to be made available to borrowers under rules of the Library.

Brief quotations from this dissertation are allowable without special permission, provided that accurate acknowledgment of source is made. Requests for permission for extended quotation from or reproduction of this manuscript in whole or in part may be granted by the head of the major department or the Dean of the Graduate College when in his judgment the proposed use of the material is in the interests of scholarship. In all other instances, however, permission must be obtained from the author.

SIGNED: Richard W. Capps

ACKNOWLEDGMENTS

A number of individuals have played key roles in the successful development and completion of this project. Without reference to their contributions, it is a pleasure to thank P. L. Capps, H. M. Dyck, F. C. Gillett, and R. F. Knacke for their willing participation. The continuous support of Kitt Peak National Observatory is gratefully acknowledged, including the efforts of R. Aikens, P. Britt, E. L. Dereniak, and R. R. Joyce.

TABLE OF CONTENTS

LIST OF ILLUSTRATIONS

LIST OF TABLES

ABSTRACT

This dissertation is an observational study of the polarization properties of a class of infrared sources which have apparent 9.7 micron silicate absorption features. In order to carry out the observations, improvements in the existing instrumentation were required. The results of this development program are contained in specific recommendations for design of a 10μ polarimeter. Detailed observations of the Becklin-Neugebauer source (BN), indicate that the linear polarization is produced by absorption in partially aligned, elongated particles. Comparison of the observations with model calculations demonstrates that the 9.7μ volume absorption coefficient of the silicate material attenuating BN is at least a factor of two smaller than laboratory values of terrestrial silicates. In addition, the characteristic size of the particles is much less than 10 microns and the index of refraction has a very small imaginary part near 10μ. Observations of six other sources imply that the degree of grain alignment around BN is high in comparison to other spectroscopically similar objects. This information is used to put constraints on various alignment processes which might operate near the infrared sources.

CHAPTER 1

INTRODUCTION

Infrared observations of the environs of HII regions and other young objects have been carried on for some time and are reviewed by Wynn-Williams and Becklin (1974). As the data have accumulated, a distinct class of objects has emerged which are characterized by the presence of a broad absorption feature around 10 microns which is usually very strong. Indications of large visual attenuation and, in varying amounts, absorption in the 3.05 micron ice band accompany the 10 micron feature. The column density of attenuating material, estimated from the apparent visual and near infrared extinction, is generally much larger than expected from the normal interstellar medium. In the case of the object in the Orion infrared cluster, estimates of the visual extinction range from about 15 magnitudes to greater than 50 magnitudes. Although the visual extinction is uncertain, it is clearly much larger than the expected 1-3 magnitudes from average interstellar conditions and a distance of 0.8 kpc.

These infrared sources with strong 9.7 micron absorption features have been found in conjuction with strong, compact radio continuum sources and also coincident with OH and H_2O masers in dense molecular clouds. In view of the high density conditions required by the large visual extinction, the association of these infrared sources with regions

of high gas density is presumably not coincidental. In fact, the attenuating dust is believed to be an important component of these molecular cloud complexes and not merely isolated concentrations along the line of sight.

The Becklin-Neugebauer source in Orion is the exemplar of these objects. Its infrared spectrum, obtained by Gillett and Forrest (1973), is reproduced in Fig. 1.1. The 9.7 micron feature, the ice band, and the rapid decrease in flux at short wavelengths are obvious. Longward of 10 microns, the associated Kleinmann-Low nebula (KL) can contribute a significant portion of the total flux. This effect is shown by the difference between the spectrum obtained with an $11\hat{''}$ field aperture. (crosses) and the one obtained with a $22\hat{''}$ aperture (dots). Although only a fraction of the known sources are associated with compact HII regions and some can be spatially resolved, we will call these objects "compact infrared sources". The name is adopted for convenience and its connotations should be applied, if at all, to the state of the attenuating dust.

The compact infrared sources are defined empirically by the presence of sufficient material to produce discernible attenuation in the 9.7 micron feature. This definition must be applied with some discretion. A number of infrared objects have absorption features which can probably be explained either by the normal conditions of interstellar medium or by the unusual character of the object. For instance, the highly reddened star, VI Cyg No. 12, has a weak 9.7 micron feature which is apparently the result of normal interstellar extinction (Reike, 1974;

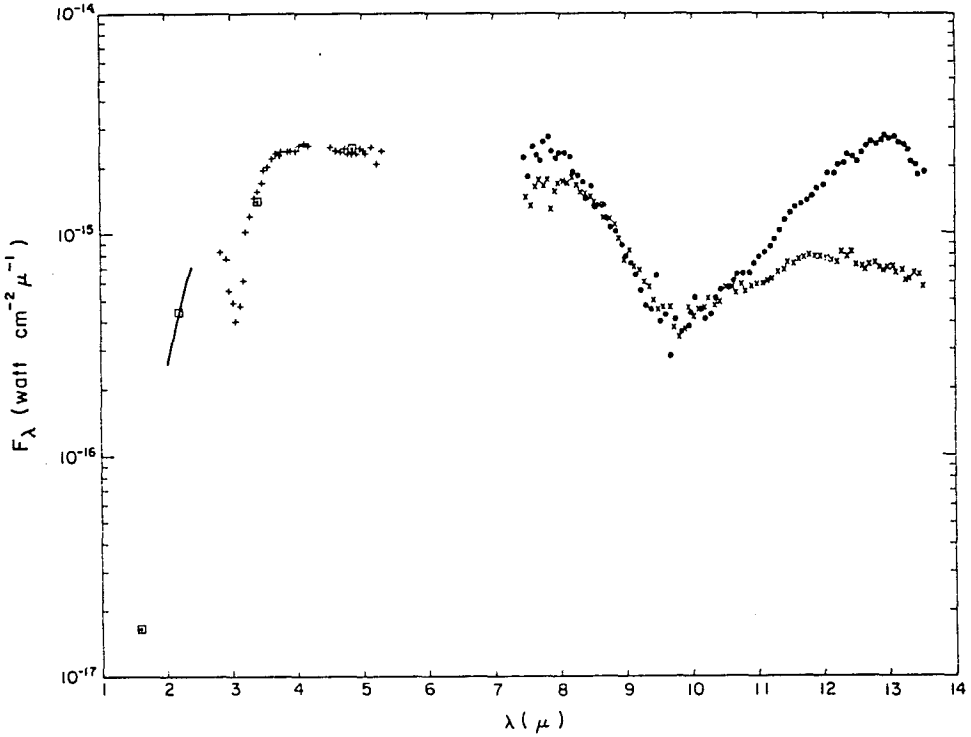

Fig. 1.1. Infrared Spectrum of BN-KL.

Crosses are data taken with an 11 $\hat{n}$ field aperture, dots are taken with a 22 in. aperture.

Gillett, Jones, Merrill, and Stein, 1975). The infrared emission from the nuclei of a number of galaxies also shows an absorption at 9.7 microns (Gillett, Kleinmann, Wright, and Capps, 1975; Kleinmann, Gillett, and Wright, in press). The spectra are similar to those of low excitation planetary nebulae such as BD +30 3639; and are reasonably distinct from the absorption features associated with galactic dark clouds. The infrared sources at the center of our galaxy have strong 9.7 micron absorption features as well (Woolf, 1973; Aikens and Jones, 1973). They provide an ambiguous situation which will be discussed in subsequent chapters.

In general, this work is concerned with investigating the properties and environment of the dust which produces the 9.7 micron absorption. In particular, the approach will be to extract a portion of the information which is carried by the photons in the wavelength region of the 9.7 micron feature by a combination of spectroscopic and polarimetric techniques. Since the perfection of infrared observing equipment and techniques is far from complete, a significant part of this program has involved the development of equipment which is sufficiently sensitive to obtain the required data. This part of the work will be outlined in the next chapter. The remainder of this introduction will be concerned with establishing the motivation for the project and a framework within which to interpret the observations.

Observations of the Compact Sources

The previously cited review by Wynn-Williams and Becklin indicates the volume of observational material which has been obtained from

infrared sources associated with young galactic objects. Of primary interest here, are the spectroscopic and polarimetric observations of the compact sources.

Spectroscopy

Detailed spectroscopic studies of the compact sources have been carried out by Gillett and Forrest (1973), Merrill and Soifer (1974), Gillett, Forrest, Merrill, Capps, and Soifer (1975, hereafter referred to as GFMCS), and Gillett and Capps (in preparation). The identification of the material which produces the 9.7 micron feature stems from the shape of the band. It is similar to the band that is seen in emission around evolved oxygen rich stars and in the Trapezium region of the Orion Nebula (Stein and Gillett, 1969). Based on observations of such stars and the calculations of Gaustad (1963), Woolf and Ney (1969) tentatively identified the absorbing material as silicate grains.

Attempts to connect the shape of the absorption band with the absorption bands of terrestrial minerals has been of limited success. Unlike other materials, silicate minerals have strong absorptions in the proper wavelength range. However, crystalized silicates, such as olivene and enstatite, have excessive spectral structure in their 10 micron bands (Zaikowski, Knacke, and Porco, 1975). These authors find that the spectral structure of hydrous silicates from type I carbonaceous chondrites and phyllosilicate minerals is much smoother than the crystallized forms of silicate. Day (1974) has synthesized an amorphous form of silicate which does produce a broad absorption feature that is very similar to that observed, but he has yet to determine the mass absorption

coefficient of the material. The identification of the 9.7 micron band with absorption from silicate material appears firm. However, because of the range of possible compositions of the material and the unknown influence of the particle structure, the mass absorption coefficient of the interstellar material is very uncertain. At best, it can be estimated from the range of measured laboratory values.

The mass absorption coefficient of the material provides the connection between the spectroscopic observations and the column density of the silicate grains, as well as insights regarding the grain structure and composition. When combined with a model of the mass distribution, it is also possible to determine the mass of silicate dust in the dark clouds. In the case of stars such as VI Cyg No. 12, the observations combine with the absorption coefficient to provide an estimate of the relative abundance of silicate material in the interstellar medium--a result which is critical in the evaluation of theories of grain formation. Because of the uncertain connection between laboratory materials and interstellar grains, we need a direct measurement of the absorption coefficient of the silicate material as it exists in interstellar space.

As part of a procedure to model the spectra of the compact sources associated with HII regions, GFMCS have generated a relative opacity law for the 9.7 micron silicate feature from observations of the Trapezium emission. They assume that the Trapezium source is optically thin and isothermal. Therefore, the relative opacities have the form,

$$\tau_\lambda = \frac{F_\lambda(\text{trap})}{B_\lambda(T_{\text{trap}})} \qquad (1.1)$$

where $F_\lambda(\text{trap})$ is the relative flux from the Trapezium and $B_\lambda(T_{trap})$ is the blackbody function for the temperature of the Trapezium dust. The value of T_{trap} is a free parameter of the model, but is required to be the same for all compact sources. The rest of the model assumes that the absorption feature is produced by a slab of non-emitting silicate grains with the opacity law of Eq. (1.1) and that the underlying source is either a blackbody (Model I) or an optically thin, Trapezium-like source (Model II).

The GFMCS model calculations yield accurate reproductions of the observed spectra of six compact sources. Forgel and Persson (to be published) have had similar success with the same basic model in fitting their observations of compact HII regions. The model fits provide us with a simple but useful description of the source structure, estimates of the temperature of the radiation source, the range of silicate optical depths, and an opacity law for the silicate grains. These results are combined with radio observations of the associated molecular clouds and HII regions and also estimates of the distances and silicate absorption coefficient to yield the following picture of the compact sources.

The sources consist of an ionizing star(s) at the center, surrounded by a small HII region and a shell of cold gas and dust. The infrared radiation source is characterized by a temperature between 200°K and 500°K and an overlying silicate optical depth of between 1 and 4, depending on the model. The radio data indicate that the total mass of the average cloud is greater than 10^5 $M_\odot$. GFMCS find that the density at the inner edge of the cold dust shell in approximately $n(H_2)$ = 10^5 cm^{-3}. The compact sources, such as BN, which are not in association

with detected HII regions are assumed to have simular structure and conditions, except for the absence of a detectable ionized region surrounding the central source.

Polarimetry

In general, stars which show excess infrared emission from heated circumstellar material are intrinsically polarized at short wavelengths (Dyck, Forrest et al., 1971; Dyck, Forbes, and Shawl, 1971; Capps et al., 1973). However, among the observed sources with 10 micron silicate emission features, none are significantly polarized around 10 microns (Capps and Dyck, 1972). This result includes objects such as VY CMa, NML Cyg, and IRC+10216 which are highly polarized in the visible and near infrared. Somewhat unexpectedly, 10 micron polarimetry of BN revealed that it is linearly polarized by more than 10% near 10 microns (Dyck et al., 1973). In particular, the polarization is largest at wavelengths in the silicate absorption feature and relatively small outside the silicate band. The polarization also increases toward short wavelengths, reaching 20% at 2.2 microns. The observed wavelength dependence of polarization is plotted in Fig. 1.2. In addition to large linear polarization, Serkowski and Reike (1973) detected circular polarization at 3.5 microns.

Scattering from the circumstellar dust is believed responsible for producing the polarization of stars with silicate excesses. Therefore, the unique wavelength dependence of polarization of BN suggested that a mechanism other than scattering produces the polarization.

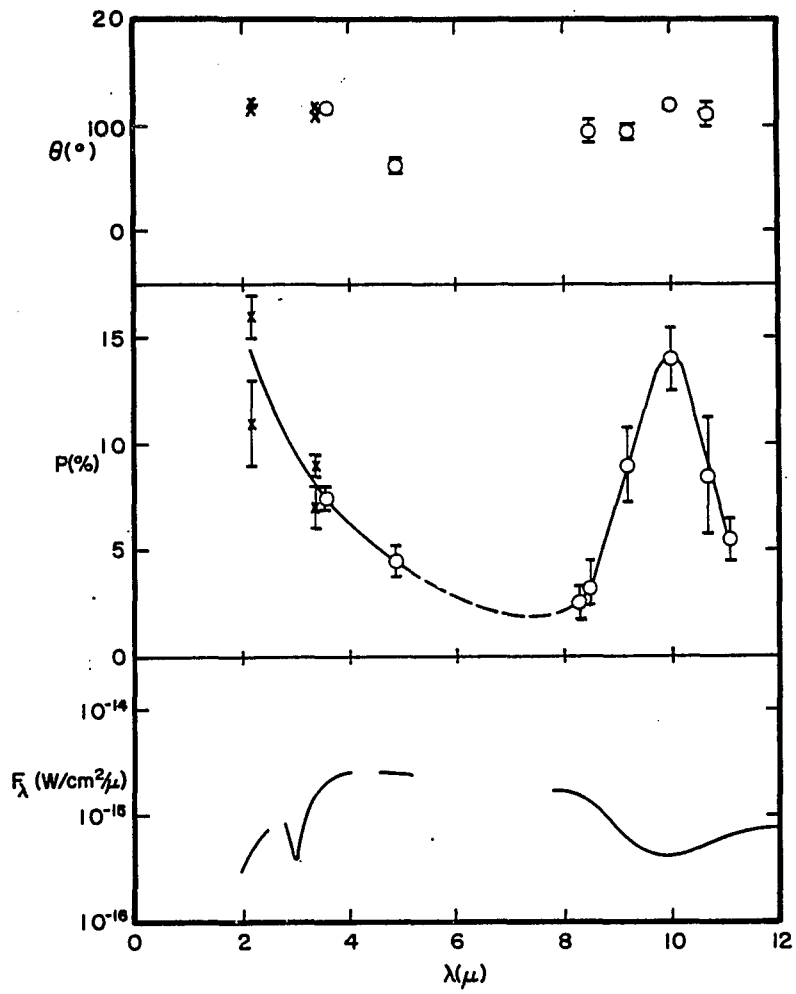

Fig. 1.2. Relation of Linear Polarization and Flux of BN.

The alternative mechanisms are discussed qualitatively by Dyck and Beichman (1974), hereafter referred to as DB. They conclude that the approximate correlation of the polarization and absorption optical depth of the silicate band requires that the polarization be produced by the dichroic absorption process.

Dichroic absorption occurs when an absorbing medium is composed of partially aligned, optically asymmetric particles. When light passes through such a medium, one plane of polarization is attenuated more than all others, resulting in partial polarization of the transmitted beam. Martin (1975) has studied the dichroic absorption process as applied to the 9.7 micron silicate feature. He finds that the wavelength dependence of the ratio of polarization and optical depth is strongly dependent on the absorption coefficient of the grains. Using existing observations, Martin found that the dichroic absorption process required that the volume absorption of the BN grains be much smaller than the laboratory values for pure silicates. In view of the possibility of providing a direct measurement of the grain absorption coefficient, we require a definitive test of the dichroic absorption mechanism. We also require improved observational data, in order to verify Martin's initial results.

Polarizing Mechanisms

Linear polarization of thermal radiation can be produced by three general mechanisms. They are scattering, dichroic absorption, and dichroic emission. We wish to consider the wavelength dependence of polarization near a solid state absorption which would be produced by each of these mechanisms. The goal is to devise a test for the dichroic

absorption process. We will assume that solid particles produce the polarization, but that they are not necessarily small compared to the wavelength.

Scattering

The case of circumstellar polarization produced by single Mie scattering has been studied in complete geometrical generality by Shawl (1972). He finds that the polarization can increase or decrease with extinction optical depth. The difference is determined primarily by whether the increased attenuation of the scattered photons is compensated by the larger solid angle of the scattering geometry compared to the direct, i.e., unpolarized, flux from the central source. Polarization from spherical particles requires a net asymmetry in the scattering geometry. However, scattering by partially aligned, non-spherical particles can produce similar results without the requirement of an asymmetric scattering geometry. They are also capable of polarizing the direct radiation from the source, which is not possible with spherical Mie particles (Greenberg, 1968).

An excellent example of polarization which is due to scattering and which increases with increasing extinction is provided by CRL 2688 (The Egg Nebula). This object is discussed by Ney et al. (1975). It consists of a central star which is surrounded by an irregular cloud of attenuating material. The visual attenuation of the cloud is large along the direct line of sight to the central source and relatively small along two transverse directions. In the visible and near infrared, CRL 2688 appears to be a pair of reflection nebulae which are produced by

scattering along the weakly attenuated transverse paths through the cloud. The polarization of the scattered radiation is greater than 30%. At 10 microns, the attenuation of the cloud is greatly diminished because the particles are small compared to the wavelength. The object appears as a single source which is centered between the positions of the reflection nebulae. It is unpolarized at 10 microns.

It is clear that polarization which is produced by scattering can increase with increasing attenuation; however, we must consider how it will behave near an isolated absorption feature. The scattering cross section of solid particles is a combination of the real and imaginary parts of the index of refraction. For instance, in the Rayleigh approximation, Van de Hulst (1957) shows that

$$C_{sca} \propto (m^2-1)^2 = (n^2-k^2-1)^2 + 4n^2k^2 \ , \qquad (1.2)$$

where n and k are the real and imaginary parts of the index of refraction, m. Far from an absorption feature, k is zero in pure dielectrics and n has a slowly varying background value of n_o. In the region of an absorption feature, n undulates about its background value and k increases considerably. Because of its dependence on k, the scattering cross section will increase in an absorption feature; however, it returns to the value determined by the background refractive index outside the absorption band wings. For this reason, polarization which is produced by scattering can increase in an absorption feature, but it will not go rapidly to zero outside of the band.

Absorption

The dichroic absorption mechanism, which is discussed by Van de Hulst (1957), requires a medium of grains which are partially aligned and which display variations in their absorption cross section as a function of electric vector orientation. For such a medium of particles, the polarization is given by,

$$P = \frac{e^{-\tau_l} - e^{-\tau_r}}{e^{-\tau_l} - e^{-\tau_r}} \tag{1.3}$$

where l and r are orthogonal directions which describe the alignment directions. For small polarizations, this expression reduces to

$$P \propto \frac{C_l - C_r}{C_l + C_r} \tau_{abs} \tag{1.4}$$

where C_l and C_r are the orthogonal grain cross sections and τ_{abs} is the absorption optical depth of the medium. Except for small variations in the relative orthogonal grain cross sections, the polarization varies in proportion to the optical depth. Once again, in the Rayleigh approximation,

$$\tau_{abs} \propto C_{abs} \propto -\mathrm{Im}(m^2-1) = 2nk \ . \tag{1.5}$$

For a pure dielectric, the polarization will tend to follow k across the band and go to zero outside the band. However, if the grain material is not a pure dielectric, the value of k, and therefore P, may not reach zero outside the band.

Emission

The possibility that infrared radiation from grains might be polarized by dichroic emission has been suggested by Stein (1966). This mechanism is the emission analog of dichroic absorption. A medium of aligned emitting dichroic grains will produce polarized flux of the form

$$P = \frac{(1-e^{-\tau_l}) - (1-e^{-\tau_r})}{(1-e^{-\tau_l}) + (1-e^{-\tau_r})} \qquad (1.6)$$

which, in the optically thin case, reduces to

$$P \propto \frac{C_l - C_r}{C_l + C_r}(1-\tau), \qquad \tau << 1. \qquad (1.7)$$

The polarization is essentially independent of optical depth. As the optical depth becomes significant, compared to 1, the polarization decreases and goes to zero in the optically thick case.

The spectroscopic observations of BN and other compact sources suggest that the silicate band absorption is very small between 7.5 microns and 8 microns. Therefore, the presence of a scattering mechanism can be checked observationally. Using refractive indices similar to those found by Martin (1975), we see that the scattering cross section will change by about a factor of 3 between the center of the 9.7 micron feature and the nearby continuum. As a result, measurable polarization should occur between 7.5 microns and 8 microns if scattering is important. If BN is unpolarized between 7.5 and 8 microns, both scattering and continuous absorption from impure dielectric particles can be rejected. The dichroic emission mechanism is not in question because it does not produce the observed wavelength dependence of polarization.

Observations

The third chapter of this dissertation presents new polarization observations of the BN silicate feature. The spectral resolution and accuracy are sufficient to test the dichroic absorption hypothesis and obtain a direct determination of the volume absorption coefficient of the silicate grains. A few of the implied grain properties are also discussed, including limits on the grain shape and alignment.

The fourth chapter presents observations of seven additional compact sources. While not being a strong statistical sample, they do extend the generality of the BN conclusions. The physical conditions expected in the compact sources are much more restrictive on possible alignment mechanisms than in the normal interstellar medium. This is the case because the polarizing geometry is known and the large attenuation of the cloud eliminates some alignment mechanisms. Various mechanisms are considered in this context in order to evaluate the possibility that strong magnetic fields are associated with the compact sources.

The prospect of studying variations in grain composition, as reflected in the silicate absorption coefficient, and also the properties of the grain environment which control the degree of alignment are presented in the concluding chapter, along with a summary of firm results.

CHAPTER 2

INSTRUMENTATION

The first version of the infrared polarimeter used for this project was constructed by H. M. Dyck (Dyck, Forbes, and Shawl, 1971). This instrument consisted of a 10 micron, focal plane chopped, infrared photometer system which allowed insertion of a rotatable linear analyzer into the telescope beam. The instrumentation development portion of this work has consisted of improvement of the photometric sensitivity of the detector system and finding the best location for the analyzer element outside of the dewar. This approach has not produced a machine specifically designed to do polarimetry; however, it has produced scientifically valuable data and the experience necessary to proceed with specialized polarimeter development. The amount of change which has occurred in the quest for improved sensitivity can be estimated by the fact that the analyzer element is all that remains of the original system.

Photometric Sensitivity Improvements

The improvements in the photometric sensitivity and mechanical quality of the photometer-polarimeter were carried out as part of a program to produce high performance infrared systems for the inventory of visitor equipment at Kitt Peak National Observatory. The success of this effort is due to the willing support of the Observatory as a whole

and the flexible collaboration of the members of the Observatory's infrared development group. In general, the photometric sensitivity increases are the result of minimizing the background radiation seen by the detector, which is the ultimate source of noise, and optimizing the collection of signal energy with more efficient optics and better detectors.

The Kitt Peak 2.1 meter and 1.3 meter telescopes, which were used to gather the observational data, are both fitted with low background optical systems and chopping secondary mirrors. The essence of the low background optical system is contained in the requirements that the aperture of the telescope be defined by the diameter of the secondary mirror and that the only radiating surfaces within the direct field of view of the detector be the secondary mirror and the sky. The detector also sees the virtual image of the primary mirror in the secondary. The result is that the background radiation is controlled by the temperature and emissivity of the telescope mirrors and not by the portion of the field of view which would otherwise be filled by the black surfaces of the primary and secondary mirror cells. The hole in the primary mirror can be a significant source of background radiation; however, this source can be hidden behind low emissivity baffles. The alternative method of reducing the background by restricting the detector's field of view with cold baffles in the dewar is less effective because of diffraction effects that broaden the response pattern of the baffles. The chopping secondary, originally devised by F. J. Low, Lunar and Planetary Laboratory, University of Arizona, has replaced the focal plane chopper as the standard

means of modulating the signal because it offers increased flexibility in the design of the focal plane package, and reduces the number of radiating mirrors needed in the photometer.

The ability of the detector system to measure the signal energy provided by the telescope is characterized by its signal-to-noise ratio. It is maximized by attempting to minimize transmission and reflection losses and by seeking a detector with the best attainable quantum efficiency. The process of minimizing system losses tends to reduce the background radiation as well. The detector systems which have resulted from this philosophy are classified as up-looking systems. In this configuration, the optical axes of the telescope and the detector field optics are co-linear. When used as a Cassegrain instrument, the only ambient temperature surfaces within the field of view are those of the vacuum vessel window and the telescope mirrors. The focal plane of the system can be placed near the top of the dewar, which makes it compatible with guiding devices designed for visual detectors.

The detector system used for most of this work consisted of a doped silicon photoconductor mounted in an up-looking configuration and interfaced to the telescope by an automatic guider which is normally used with a visual spectrograph. The spectral response of the detector is determined by a set of filters which are cooled to approximately $60^{\circ}K$. The filter set includes passband filters which range from 3.5 microns to 12.6 microns and a 2% resolution circular variable filter which covers the range of 7 microns to 14 microns. The filter characteristics are summarized in Table 1.1.

Table 1.1. Filter Characteristics.

$\lambda(\mu)$	$\Delta\lambda(\mu)$
3.5	0.6
8.5	1.0
11.5	1.3
12.6	2.0

Infrared Linear Analyzers

The optical element which modulates the linearly polarized component of the telescope signal is the analyzer. For operation near 10 microns, one could use various polarizing prisms, "pile of plates" polarizers, or wire grid polarizers as the analyzer. The requirements that the analyzer be easily insertable in the system and operate in a moderate focal ratio beam rapidly reduces the choice to the wire grid polarizer. Additional problems are encountered when one examines the cost of 10 micron prisms, which must be built from exotic materials, and the efficienty of pile of plates polarizers.

The wire grid polarizer is, in principle, a plane surface composed of a series of parallel, perfectly conducting ribbons. Under the condition that the spacing between ribbons is both equal to their width and much less than the wavelength, the wire grid acts as a perfect polarizer. The component of the incident radiation whose electric vector is parallel to the conductors is reflected while the perpendicular component is transmitted. The performance of the polarizer is only a

weak function of the angle of incidence and refractive index of the supporting dielectric substrate. A survey of the experimental and theoretical studies of the performance of wire grids is given by Larsen (1962).

Commercially available wire grids which operate in the infrared have wire spacings as small as 0.33 microns which allows use at wavelengths as short as 3 microns. The grids are fabricated by ruling, replicating, or photo-etching grooves of the proper spacing into the substrate and then metalizing the ridges between the grooves. The Perkin-Elmer wire grid polarizer was the first marketed and has the finest ruling available. This polarizer is produced by pressing the grooves into a soft silver chloride substrate with a master grating. Unfortunately, the pressing operation appears to produce significant nonparallelism of the substrate surfaces and the material is both photo sensitive and chemically active. Eventually, the substrate grows a chemical mold which renders it unusable.

In addition to modulating the signal photons, the wire grid operates on the background photons. In the case of a background limited system, which applies at 10 microns, consideration of the polarizer's effect on the background flux is critical in achieving the optimum sensitivity of the system. In order to study this effect, let us consider an idealized infrared photometer as shown in Fig. 2.1. This photometer consists of a 10 micron detector mounted in a $4^{\circ}K$ dewar box which is in turn mounted on a $300^{\circ}K$ photometer box. This assembly is mounted on a $300^{\circ}K$ telescope. Properly sized holes in the walls of the two boxes allow the converging telescope beam to focus on the detector while not

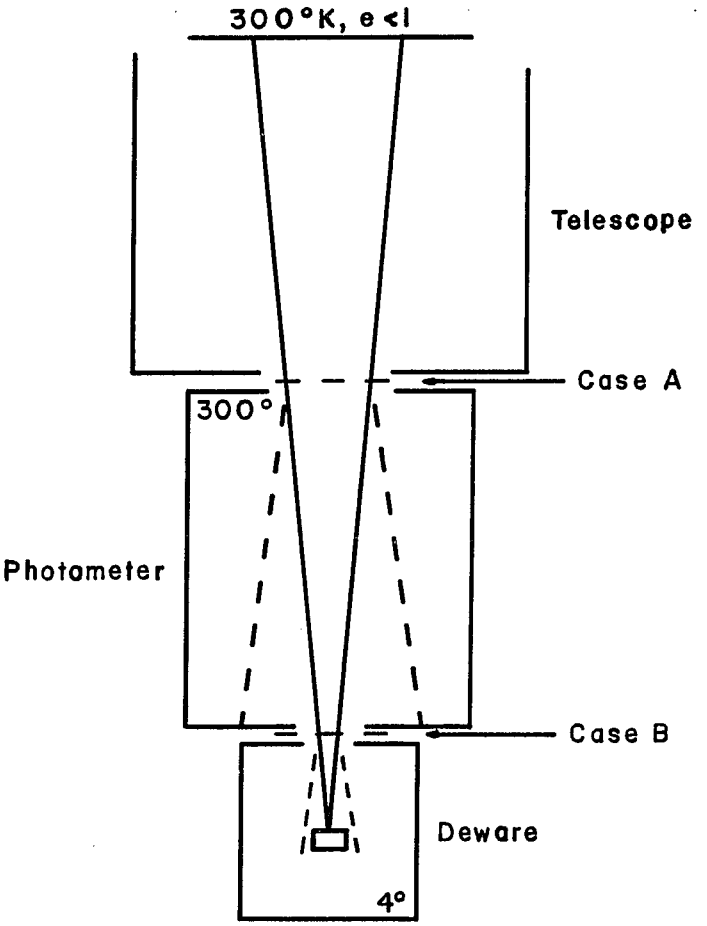

Fig. 2.1. Idealized Infrared Polarimeter.

allowing the detector to see the walls of the 300°K box. In this arrangement, the background flux is produced by emission from the telescope optics, which the detector can see, and not by the walls of the photometer. If the effective emissivity of the telescope is e, then the background on the detector will be proportional to this emissivity times the appropriate blackbody function.

$$P_t \propto eB(300^\circ K), \qquad e<1 \ . \tag{2.1}$$

The constant of proportionality is the product of the area of the detector, the solid angle of the telescope beam, the optical bandwidth and a transmission factor. Suppose the telescope is pointed at an unpolarized infrared source which produces a signal level, R, on the detector. If R is much smaller than P_t the signal-to-noise ratio has the form

$$(S/N) \propto R/\left[eB(300^\circ K)\right]^{1/2} \tag{2.2}$$

This expression demonstrates why, aside from detector improvements, working toward reduced system emissivity produced immediate sensitivity improvement. Let us consider, as case A, the result of placing a perfect wire grid polarizer in the hole between the 300°K box and the telescope. The polarizer attenuates the signal and background received from the telescope by a factor of two. In addition, the polarizer acts as a 50% reflective mirror which allows the detector to see the walls of the 300°K box. The background expression becomes

$$P_A \propto 0.5(e + 1)B(300^\circ K) \tag{2.3}$$

and this signal-to-noise ratio is then

$$(S/N)_A \propto R/\ 2(e + 1)B(300^{\circ}K)^{\frac{1}{2}} \tag{2.4}$$

Clearly, this is an undesirable result because the background is now larger than in the normal photometric case. Reducing the signal level by a factor of two is the normal price of doing polarimetry; however, increasing the noise at the same time should not be necessary. Unfortunately, the conditions of case A have been produced in a number of infrared systems, including the first one used here.

As case B, consider the result of placing the polarizer in the hole between the $4^{\circ}K$ box and the $300^{\circ}K$ box. By analogy with case A, the background radiation has the form

$$P_B \propto 0.5\left[eB(300^{\circ}K) + B(4^{\circ}K)\right] \tag{2.5}$$

but,

$$eB(300^{\circ}K) >> B(4^{\circ}K)\ . \tag{2.6}$$

Therefore,

$$P_B \propto 0.5eB(300^{\circ}K)\ . \tag{2.7}$$

The form of the signal-to-noise ratio is then

$$(S/N)_B \propto R/\left[2eB(300^{\circ}K)\right]^{1/2}\ . \tag{2.8}$$

Case B yields the optimum sensitivity for a single channel, background limited polarimeter with an external analyzer. This situation can be achieved in practice by placing the wire grid as close to the Dewar window as practical. Moving the polarizer inside the Dewar and reducing its temperature to cryogenic levels would be an even better solution. Low background telescope designs have reduced the effective

emissivity to e = 0.15 - 0.20. For e = 0.15, the possible improvement in sensitivity between case A and case B is

$$(S/N)_B/(S/N)_A = \left[(e + 1)/e\right]^{1/2} = 2.8 . \qquad (2.9)$$

Sensitivity gains using this technique are not as spectacular as predicted because of thermal emission from the polarizer substrate. This problem is accentuated by the developement of silver chloride mold on the polarizer which has an emissivity near unity. Competition among manufacturers of wire grid polarizers is starting to yield alternatives to the Perkin-Elmer device which may not have the problems associated with its substrate.

The Ten Micron Polarimeter

Modulation of the polarized component of the signal radiation is accomplished by rotating the analyzer in the telescope beam. The amplitude of the electrical signal which is produced by this modulation is proportional to the polarized flux; the signal frequency is twice the rotation frequency of the analyzer. It would be desirable to rotate the analyzer continuously and also synchronize the chopper to the analyzer. This would allow acquisition of the data at frequencies above the average rate of atmospheric and background variations. Unfortunately, this technique proved to be extremely noisy for two reasons. In the original version of the polarimeter, the analyzer was sufficiently far from the field aperture that the beam deviation associated with the non-parallelism of the substrate was larger than the field size. Continuous rotation was impossible because the image had to be recentered as a function of analyzer orientation. This problem was reduced to a tolerable level by

moving the analyzer close to the Dewar. However, as the analyzer is rotated in the field of view of the detector, radiating specks of dust and regions of variable emissivity move about in the detector beam. The noise introduced by these background variations overwhelms all other noise sources at 10 microns. Continuous analyzer rotation is possible at wavelengths where the $300^{o}K$ background noise is small compared to other noise sources.

The observing technique which has proven to be a viable compromise between the various competing problems is to measure the signal flux at eight discrete positions of the analyzer and examine these measurements for 2θ modulation. Philosophically, the adoption of this technique must be considered a step in the wrong direction. A set of observations at each of the analyzer positions, which constitutes a single polarization measurement, requires several minutes. These individual polarization measurements are collected and co-added to improve the accuracy of the integrated measurement. The success of this polarimeter requires the detection of small differences in flux measurements which are significantly separated in time. Therefore, the system is extremely sensitive to low frequency variations in its photometric environment. Usually, the data frequency was maximized by taking only one ten or twenty second integration at each of the eight positions of the analyzer. The position sequence suggested by Serkowski (1962) was used for this purpose as well. The dead time has been minimized by positioning the analyzer and sequencing the data collection with the telescope control computer.

The frequency dependence of 10 micron noise is highly variable, but usually has a 1/f component below 10 Hz. This is the reason that the signal is modulated at rates which are typically above 10 Hz. Low frequency variations in the atmospheric transmission are not removed by the chopper and are the principle noise source in the current polarimeter. The presence of low frequency variations is demonstrated by a subset of the observations which were taken with multiple integrations at each analyzer position. The absolute polarimetric and percentage photometric uncertainties of a single measurement are compared in Fig. 2.2. The filled dots follow the expected relationship of the two uncertainties. They compare the polarimetric errors with the photometric repeatability over twenty second intervals which is the time required for individual flux measurements. The open circles compare the same polarimetric errors with the photometric repeatability over five minute intervals. The degradation of the photometric noise is obvious. The polarimetry is limited by the twenty second repeatability of the system, which is worse than the background noise limit for bright sources. Thus it appears that significant improvement will accompany faster polarization measurements.

The data reduction procedure has been described previously by Knacke and Capps (1974) and is explained in detail in Appendix A. The procedure consists of determining the normalized linear Stokes parameters of the program objects and unpolarized standard stars at each wavelength. The correction for polarization produced by the instrument is made by subtracting the average standard star Stokes parameters from the program measurements. The position angle correction is determined following the method of Gehrels and Teska (1960). This involves measurement of a

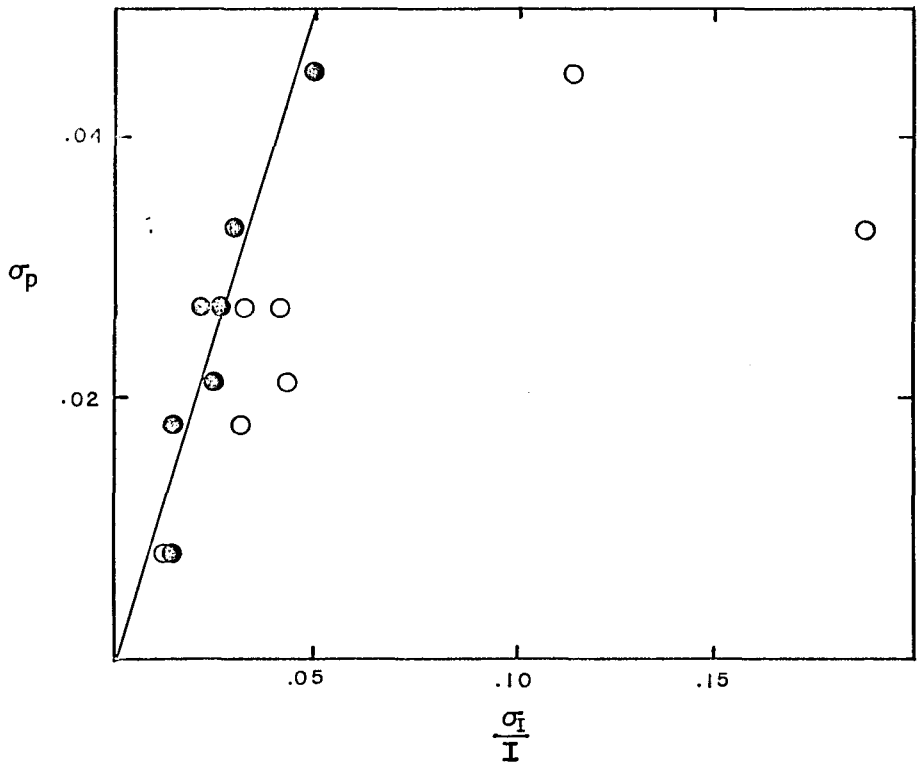

Fig. 2.2. Comparison of the Fractional Photometric Uncertainties with the Absolute Polarimetric Uncertainties.

$\frac{\sigma_I}{I}$ is the fractional photometric uncertainty, and σ_p is the absolute polarimetric uncertainty.

bright source through a reference polarizer whose orientation in the telescope beam is known. Measurements through a pair of wire grid polarizers indicate that their polarizing efficiency is greater than 0.98. Therefore, no correction is made for incomplete modulation of the polarized flux.

The instrumental polarization was generally found to be less than 1.5% at all wavelengths except 3.5 microns. The instrumental polarization could be produced by the telescope mirrors, the interference filters, the field optics, or the detector. Because of the high reflectance of typical mirror coating materials at infrared wavelengths, the expected level of polarization from the telescope and field optics is negligible. The portion of the instrumental polarization produced by the filters between 8 microns and 13 microns, including the circular variable filter, is apparently small. This conclusion was reached because major changes in the magnitude and direction of the system's polarization occurred when the detector was changed. Detector changes were a frequent occurrence because the system was also used to evaluate the performance of a number of different photoconductors during the period that the observations were made. Apparently, these photoconductor detectors are slightly polarized. This is probably related to the transverse electric field of 100 V cm^{-1} to 500 V cm^{-1} which is required to bias the detector. The instrumental polarization at 3.5 microns changed from 3% to 1% and then back to 3% over a one-year period. Apparently the 3.5 micron instrumental polarization is produced by the filter; however, this could not be clearly demonstrated.

Future Ten Micron Polarimeters

Based upon the experience gained from using the discrete orientation polarimeter, it is possible to specify the requirements for a specialized 10 micron polarimeter. It is clear from the discussion of the properties of the analyzer that is should be capable of reducing the background along with modulating the signal. In addition, the analyzer, or a wave plate in the detector beam, cannot be in motion during the measurement. Finally, in order to minimize atmospheric effects, individual polarization measurements must be made rapidly. One possibility which satisfies these requirements is a system similar to that described by Angel and Landstreet (1970a, 1970b), which uses a Pockels cell to achieve rapid modulation of the polarized flux. The fabrication of a cuprous chloride (CuCl) modulator which is useful in the wavelength range 0.4 micron to 20 micron is discussed by Sterzer, Blattner, and Miniter (1964). They point out that CuCl has advantages over dihydrogen phosphate modulators because it has a much wider acceptance angle. Unfortunately, difficulty in producing optical quality crystals of adequate size has precluded commercial production thus far. As an alternative, a photoelastic modulator might be substituted for the Pockels Cell (Kemp, 1969). The principle difficulty associated with this device is its high modulation frequency. Under low background conditions, even fast 10 micron detectors do not operate well above 1000 Hz. Typical operating frequencies are below 100 Hz. The photoelastic modulator operates most efficiently at the natural frequency of

the optical element. This frequency tends to be above 50 KHz. Modulation at low frequencies is produced by beating two modulators whose difference frequency is in the desired range. Kemp (1976) has achieved successful operation of such a modulator; however, the importance of reflection losses from the high refractive index material and the level of background radiation resulting from the power dissipation in the element have not been evaluated. A major advantage of the birefringent modulator design rests in its ability to easily measure circular polarization. It is envisioned that the linear analyzer which follows the modulator in this design would be mounted in the detector Dewar and cooled to at least 77^{o}K.

A second design which appears to meet the general requirements of a high performance 10 micron system is generally classified as a dual channel polarimeter. Such instruments have been used successfully at visual wavelengths. Usually, the device which divides the beam into two orthogonally polarized components is a Wollaston prism. Such prisms can be fabricated to operate at 10 microns; however, the choice of birefringent materials is limited and relatively poor transmission is to be expected. In order to satisfy the requirement of reduced background, the prism must be cooled. The effect of the mechanical stresses associated with thermal cycling of the prism is unknown, but is likely to be detrimental. In principle, there is a good alternative to the polarizing prism as a beam divider. This alternative is contained in an unexploited property of the wire grid polarizer. Unlike absorption polarizers, the orthogonal components of the radiation are either transmitted or reflected by a wire grid. It seems reasonable to expect that

a successful dual channel polarimeter can be developed with a cooled wire grid as the beam divider. The problem of cross-talk resulting from reflection from the substrate can be minimized by inserting the polarizer into the beam at the Brewster angle of the substrate. One detector is used to collect the transmitted energy and a second is used to collect the reflected energy. A dual channel polarimeter measures one Stokes parameter at a time. Measurement of the second Stokes parameter is accomplished by either rotating the detectors by 45 degrees in the telescope beam or feeding the detectors with a half wave plate which is rotated 45 degrees between measurements. Gain differences in the two channels are eliminated by additional rotations which cancel the differences. Should the 10 micron birefringent modulator be perfected, the ultimate system for measuring both linear and circular polarization may be a marriage of the modulator and the dual channel linear polarimeter. The question of whether the expected scientific discoveries justify the development of such a polarimeter remains to be answered.

CHAPTER 3

THE BECKLIN-NEUGEBAUER SOURCE

The feasibility of obtaining improved 10 micron polarization observations of BN was demonstrated in January of 1975 with the KPNO closed cycle cooler spectrometer-polarimeter. This system, which is an "up-looking" configuration, was used on the 2.1 meter telescope to obtain linear polarization measurements of BN at 0.5 micron intervals between 8 microns and 13 microns with a spectral resolution of 2%. Additional measurements were obtained with the same system during the period of October 14-17, 1975, and on November 14, 1975. These measurements are presented in Fig. 3.1. A 10.5 ″ field aperture was used and the chopper throw (35-40 ″), was sufficient to avoid other sources in the region. βPeg and αTau were used as standard stars to determine the instrumental polarization at each position of the filter wheel. The combined data covered the range from 7.4 microns to 13 microns with a spacing between data points approximately equal to the spectral resolution. The largest uncertainties in the magnitude of the polarization, which occur at wavelengths where the combined attenuation from the silicate band and the atmospheric ozone is large, are less than 1 percent polarization (1σ).

The use of a 10.5 in. field aperture was necessary to reduce the noise associated with small guiding errors and bad seeing to an

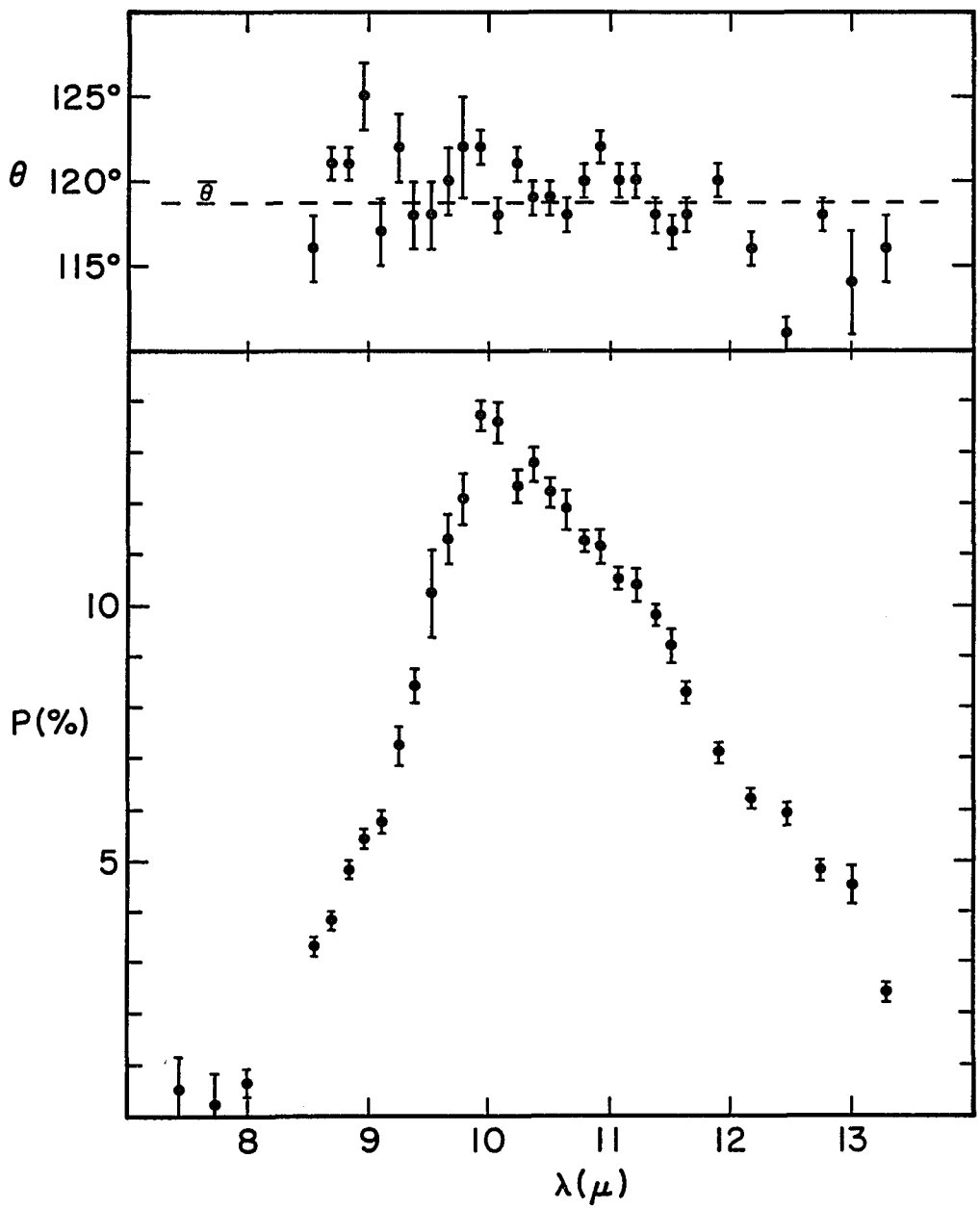

Fig. 3.1. Linear Polarization Observations of BN.

acceptable level. This admits the possibility of contamination from the emission of the Kleinmann-Low nebula at wavelengths longward of 11.5 microns. Filter wheel measurements between 12.45 microns and 13.3 microns show that the change in signal between a 7 $\hat{''}$ aperture and a 10.5 $\hat{''}$ aperture is no more than 10% greater than the change found for a point source. Since the KL flux is polarized in the same direction and approximately the same amount as BN (DB), the contribution of KL to the measured flux of BN is not important in the analysis of the observations.

Inspection of Fig. 3.1 reveals some interesting properties of the data. The polarization is sharply peaked and reaches a maximum at 9.9 microns. This peak is clearly displaced relative to the center of the absorption feature at 9.7 microns. There is a slight indication of rotation in the position angle with wavelength; however, it is not supported by the statistics of the data. Assuming there is no rotation, the standard deviation of a single point is 2.8 degrees, which is comparable with any possible rotation. This value is determined from the real scatter in the data.

The verification that the polarization is very small between 7.5 microns and 8 microns lends support to the arguments of DB that the polarization is produced by linear dichroism of the silicate grains. In this model, the polarization results from pure absorption by partially aligned, elongated grains which are much smaller than the wavelength of the absorbed radiation. As discussed previously, the alternative is to produce the polarization by scattering from particles which are not

small, compared to the wavelength. Since the scattering cross section depends upon both the real and imaginary parts of the index of refraction, polarization would be expected outside the silicate band under such conditions. The presence of significant polarization at 13 microns is not a contradiction because the absorption band is probably skewed toward long wavelengths (GFMCS). The shift of the polarization maximum away from the band center is also a product of the linear dichroism mechanism which was pointed out by Martin (1975). Since the dichroic absorption model has successfully explained the previous results and is compatible with the general features of the data presented here, it is reasonable to adopt it as a working hypothesis.

Internal Grain Properties

Following the expression of Aannestad and Purcell (1971) Eq.1.3, the relation between polarization and extinction optical depth, τ, becomes

$$P(\lambda) = 0.5 \cos^2(\psi)\, Q_A S(\lambda,R) \tau(\lambda) \ . \qquad (3.1)$$

Q_A is the alignment parameter defined by Purcell and Spitzer (1971), which is equal to 1.5 times the corresponding parameter F introduced by Davis and Greenstein (1951). The factor $S(\lambda,R)$ is the polarizing efficiency of the grain and is given by

$$S(\lambda,R) = (C_l - C_r)/\overline{C} \ . \qquad (3.2)$$

S is the difference in the extinction cross sections of a grain for radiation whose E-vector is alternately parallel or perpendicular to the grain's symmetry axis, divided by the mean cross section for the grain. This factor contains the dichroic properties of the grain which are parameterized by R, the axial ratio. ψ is the angle between the alignment direction and the plane of the sky. The relation between P and τ is valid as long as $P << 1$, an approximation which might be called "polarimetrically thin". As long as P is small, this approximation is correct even though τ may be large.

Equation (3.1) demonstrates the qualitative proportionality of P and τ which was observed by Dyck et al. (1973), provided S is not strongly wavelength dependent. In detail, however, the wavelength dependence of the ratio of P and τ is determined by the variations in S. Martin (1975) has examined the behavior of S for a variety of absorption coefficients and grain geometries. He finds that P/τ is a sensitive function of the band's absorption coefficient and is useful in estimating the grain's shape and alignment. The results of this study are consistent with the work of DB, without being constrained by the need for measured optical constants. The generality of Martin's resonance model is highly desirable in testing the dichroic absorption hypothesis. In view of the substantial improvement in the polarization data and refinements in the spectroscopic results, a comparison of the observations with the model predictions should provide a conclusive test for dichroic absorption.

The resonance model takes the form of an algorithm which generates the complex index of refraction of hypothetical grain material by requiring that it reproduce the observed opacity law. Following Martin's techniques, a two resonance fit to the 9.7 micron band's opacity law was generated via the dispersion relations and the appropriate expression for the mean absorption cross section of the grains. The complex index of refraction, $m = n - ik$, is given by

$$m^2 - 1 = 4\pi \frac{e^2}{m} \sum_j \frac{Nf_j}{\omega_j'^2 - \omega^2 + i\,\gamma_j\omega} + m_o^2 - 1 \qquad (3.3)$$

and

$$\omega_j'^2 = \omega^2{}_j - \frac{4\pi}{3} \frac{e^2}{m} Nf_j \qquad (3.4)$$

The frequencies, ω_j, damping constants, γ_j, and relative strengths, f_2/f_1, of the resonances determine the shape of the band (Longhurst, 1967). The oscillator strength of the principle resonance remained a quasi-free parameter which was used to vary the absorption coefficient. The value of the background refraction index, m_o, was chosen to be 1.5 by Martin. This value is typical of silicate minerals and is used here also. The opacity law was taken from the work of Gillett and Capps (in preparation). It was derived in the same fashion as the previous version by GFMCS, except the observations of the Trapezium are used to fit the spectrum of NGC 2024 #2 rather than a group of compact sources. This change is considered an improvement because the intrinsic spectrum of NGC 2024 #2 is believed to be that of a $10^{4\circ}$K blackbody. Knowledge of the underlying spectrum allows a check of the consistency of the fit,

which is not possible otherwise. The change in the opacity law is parameterized by a small change in the Trapezium dust temperature.

For isotropic spheroids which are small compared with the wavelength ($x = 2\pi a/\lambda << 1$, a = long axis of the grain) and whose index of refraction is not large ($|mx| << 1$), the two cross sections, C_l and C_r, due to absorption are given by Van de Hulst (1957) as

$$C_{l,r} = (2\pi V/\lambda)\mathrm{Im}\{(m^2 - 1)/[L_{l,r}(m^2 - 1) + 1]\} \quad (3.5)$$

where V is the volume of the grain, m is the complex index of refraction, λ is the wavelength, and L_l and L_r are analytic functions of the grain shape. In order to avoid specifying the grain's size, the volume absorption coefficient, k_v (cm^{-1}) is calculated. The mass absorption coefficient, κ , is the volume absorption coefficient divided by the grain density.

In order to calculate the mean cross section of the grain, the distinction between oblate and prolate grains must be considered (Martin, 1975). Oblate grains that are rotating about their short axes and aligned in the plane of the sky have

$$\bar{C} = 0.5(C_l + C_r) \quad (3.6)$$

while for prolate grains which are also rotating about their short axes,

$$\bar{C} = 0.25(C_l + 3C_r) \quad . \quad (3.7)$$

The shape of the grain is important in determining the level of polarization because the polarizing efficiency of oblate grains is twice that

that of prolate grains. However, when S is normalized, the wavelength variations are only weakly dependent on the shape. Therefore, the compromise mean cross section of Aannestad and Purcell (1971) is used here,

$$\overline{C} = (C_l + 2C_r)/3 \ . \tag{3.8}$$

The wavelength variations in S result from the fact that C_l peaks at a slightly longer wavelength than C_r. The separation of the two peaks is primarily dependent upon the absorption coefficient of the grain, rather than its shape. When the grain is exposed to an electric field, dipoles are induced in the material. Since the grain is small compared to the wavelength, the external field is uniform over the grain. The restriction that $|mx| << 1$ insures the static polarization is established in a time which is short compared to the period of the external field. With this condition satisfied, the internal field is the vector sum of the external field and the "depolarization field" of the induced surface charges (Kittell, 1971). The depolarization field is proportional to the displacement of the charges in the material and is in a direction opposite to the external field. If the dielectric material is modeled as a collection of classical oscillators, then the depolarization field contributes to the restoring force on the electrons. The resonance frequency of a small particle is therefore increased relative to the resonance frequency for the bulk material.

In order to understand the behavior of S near a resonance, we must examine the depolarization fields in an ellipsoid relative to the

same fields in a sphere. For particles of equal volume, opposite charges induced by an external field parallel to the long axis of an ellipsoid will have greater separation than opposite charges on a sphere. Therefore, relative to a sphere, the depolarization field and the resulting frequency shift will be smaller for the ellipsoid. The effect is reversed along the short axis of the ellipsoid. As the shape of the particle departs from sphericity, the maximum of C_l shifts to longer wavelengths and the maximum of C_r shifts to shorter wavelengths. When the depolarization effects are combined with the dispersion relations, the frequency difference between the two peaks can be shown to have the form,

$$\Delta\omega = [Nf(L_l - L_r)] \tag{3.9}$$

where Nf is the oscillator strength of the resonance. For a change in axial ratio of R = 1.25 to R = infinity, the quantity $(L_l - L_r)$ changes by a factor of only 2.3 for prolate grains and 3.3 for oblate grains. Therefore, the wavelength variations in S are primarily controlled by the oscillator strength, which also determines the value of the absorption coefficient.

The values of P/τ for BN were calculated using the same opacity law to which the resonance model was fit. In order to eliminate the value of the central optical depth from the analysis, P/τ was normalized to unity at 11 microns. These values are compared with a similarly normalized set of S curves in Fig. 3.2. Since the peak wavelength of the model's opacity law is dependent upon the absorption

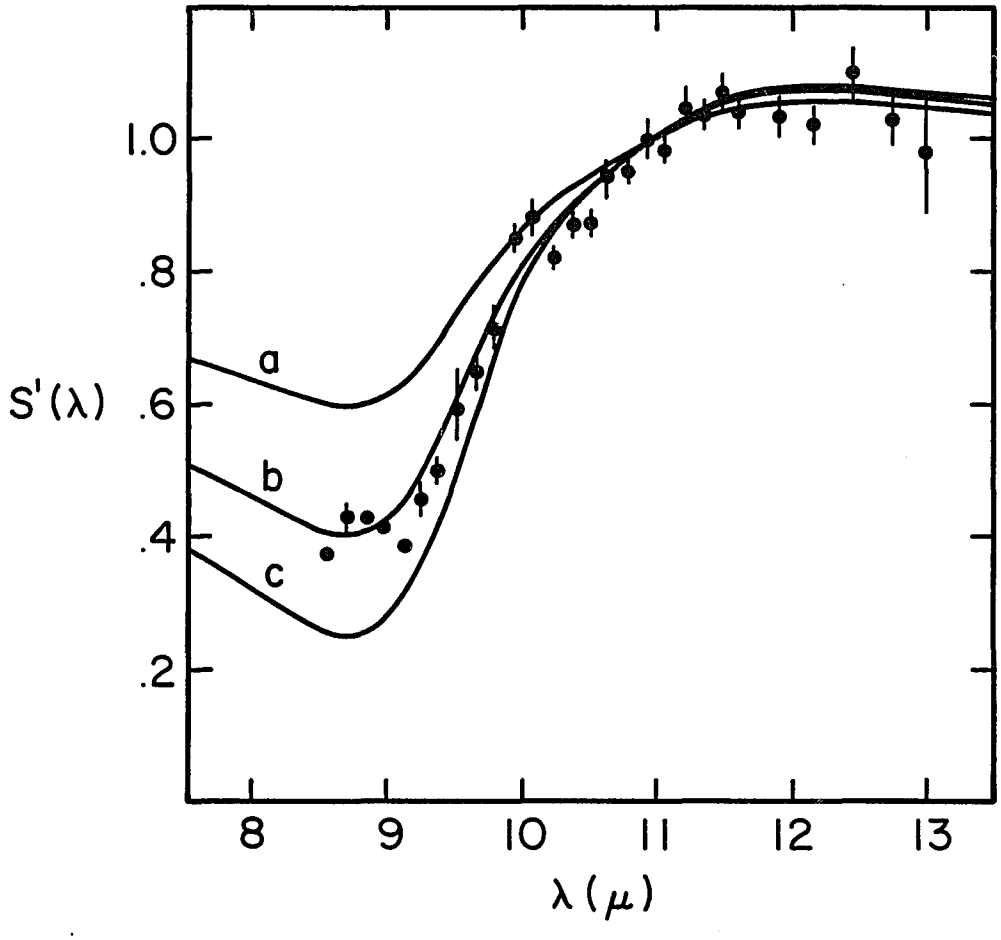

Fig. 3.2. Comparison of Normalized Observations of P/τ for BN with Normalized Model Calculations of $S(\lambda)$.

coefficient, a simultaneous fit to the opacity curve required iteration of the model parameters. The fit to the opacity law is displayed in Fig. 3.3. Reasonable fits occur for curve b in both figures. Curve b requires a peak volume absorption coefficient of $k_v = 4.8 \times 10^3 cm^{-1}$. Curves a and c, corresponding to $k_v = 2.9 \times 10^3 cm^{-1}$ and $k_v = 6.7 \times 10^3 cm^{-1}$, respectively, demonstrates the range of values which are compatible with the observations and also the sensitivity of the model to small changes in the absorption coefficient. Changes in the grain axial ratio from R = 2 to R = 5 produce displacements of the curves which are approximately equal to the size of the data points. An independent limit on the peak volume absorption coefficient occurs at a value of $k_v = 1.0 \times 10^4 cm^{-1}$. Larger values produce negative polarization at about 8.8 microns. This would manifest itself as a discontinuous 90^o rotation of the position angle at that wavelength, which is not observed. The best fit value of the mass absorption coefficient is a factor of 1.5 larger than the value obtained by Martin. This is not particularly surprising in view of the quality of the data he was forced to use.

The analysis of the polarization data could underestimate the absorption coefficient if a portion of the observed polarization was due to other than silicate grains. In order to change the results, this component would have to be present at 8.5 microns. The detection limit at wavelengths short of 8 microns is 2%. Most of this upper limit is required to account for the polarization expected from the model. Therefore, the probable limit on a non-silicate component is

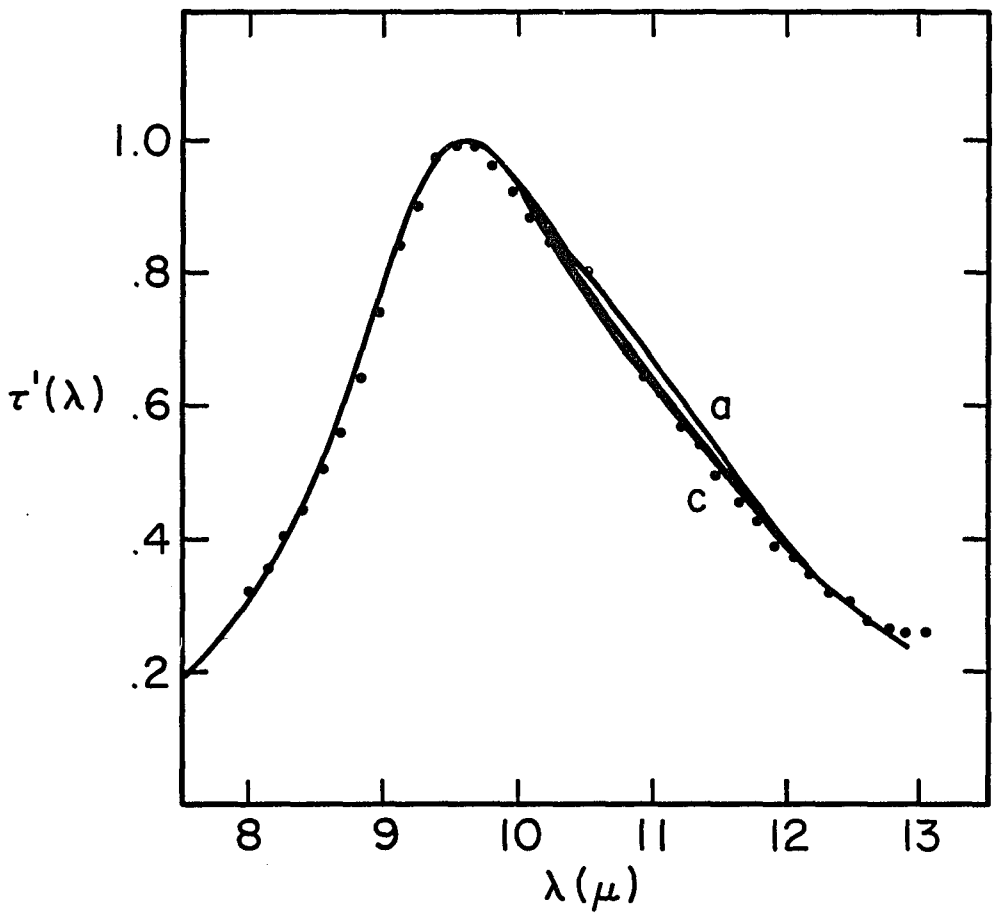

Fig. 3.3. Consistency of Observed and Calculated Silicate Opacity Laws.

less than 1%. Even if the polarization between 8 microns and 9 microns were reduced by 0.02, the volume absorption coefficient could be raised to only $9.0 \times 10^{3} cm^{-1}$ which is still below the pure silicate values. The presence of a neutral polarization component in the data would be revealed as an excess in P/τ between 12 microns and 13 microns. The same arguments also restrict the possibility of a small imaginary part of the background index of refraction which would produce polarization outside the band. Model calculations which include a small imaginary part of the background index show that it cannot be larger than 0.02. The ability of the dichroic absorption model to account for the polarization in the band wings is probably its strongest test. There does not appear to be any significant discrepancies between the model and the observations. The fits to the observations occur for $|m| < 2$. As long as the particle size is typical of interstellar grains ($a < .1$ micron), the conditions of the Rayleigh approximation are satisfied. Although the scattering geometry does enter the problem, the absence of polarization outside the band suggests that the scattering is very small and that the grains are, indeed, much smaller than 10 microns.

Gillett, Jones, Merrill, and Stein (1975) discuss the current state of laboratory absorption data for silicate material. There are some inconsistencies between Mie calculations and experimental results which are probably due to saturation effects; however, they conclude that the range of acceptable peak mass absorption coefficient values for pure silicate material is between $5.0 \times 10^{3} cm^{2} g^{-1}$ and $1.0 \times 10^{4} cm^{2} g^{-1}$.

Assuming a grain density of 2 g cm^{-3}, the best fit absorption coefficient for BN is only half the value for pure silicates. This is a conservative estimate because a density of 3 g cm^{-3} may be more realistic. The lack of position angle rotation sets an upper limit for BN of $\kappa = 5.0 \times 10^3 cm^2/g$ which is also below the range of pure silicate absorption coefficients.

If the 9.7 micron absorption feature is due to known silicates, then the polarization data require that the mass absorption coefficient of the pure material be diluted in the interstellar grains. This can presumably be accomplished by mixing the silicate with other non-absorbing material and possibly by the grain structure. Lunar rocks such as 12073,42 and 1002,186, which are microbreccia--a cemented accumulation of minerals--and also carbonaceous chondrites have weaker silicate absorption bands than olivine and enstatite rocks (Zaikowski and Knacke, 1975). The structure and composition of these materials appear to provide an indication of the properties of the grain material.

Assuming that the BN grains and those of the normal interstellar medium are similar, a lower limit on the silicate volume absorption coefficient can be established. Gillett, Jones, Merrill, and Stein (1975) estimate that the minimum mass column density of grains necessary to account for the visual extinction of VI Cyg No. 12 is

$$r_{min} = 1.6 \times 10^{-4} \rho_g \text{ g cm}^{-2} \qquad (3.10)$$

where ρ_g is the grain density. They also find a lower limit on the 9.7 micron optical depth of

$$\tau_{9.7} \geq 0.5 \ . \tag{3.11}$$

Using this estimate of the silicate optical depth, the minimum column density of silicate grains is given by,

$$r_{sil} = \frac{\tau_{9.7}}{\kappa_{9.7}} > \frac{0.5}{k_v} \rho_g \ g \ cm^{-2} \tag{3.12}$$

which leads to

$$1 \geq \frac{r_{sil}}{r_{min}} \geq \frac{0.5}{1.6x10^{-4} \ k_v} \tag{3.13}$$

and

$$k_v \geq 3.1x10^3 \ cm^{-1} \ . \tag{3.14}$$

The best fit value of $v = 4.8x10^3$ for the BN grains is compatible with this limit for interstellar grains. If the BN and interstellar grains are the same, the silicate material can account for at least 65% of the interstellar extinction to VI Cyg No. 12. This value is independent of the grain density.

We have seen that the derived value of the absorption coefficient depends primarily upon the wavelength separation of the maximum absorption and maximum polarization of the silicate band. It is unclear how important the overall shape of the opacity law is in fitting the polarization. The opacity law itself was determined empirically and its validity is measured by the number of 10 micron spectra of compact sources which it can reproduce under the assumptions of GFMCS models. The shape of the opacity law is fixed by the temperature assigned to

the Trapezium dust, which is a free parameter in the fitting procedure. The best fit value of T_{trap} is found to be 250°K. This temperature is a parameter of the model and, as yet, has no strong physical basis. Assuming that the inflection point of the opacity law is well determined, we can use it and the absorption coefficient in a modified fitting procedure which examines the range of band shapes which are compatible with the polarization data.

The results of a series of such fits are contained in Figs. 3.4 and 3.5. The polarization is normalized at λ_{max} in order to eliminate the central optical depth. The errors in the polarization data are used to establish an envelope of allowable polarization curves and corresponding opacity laws. The volume absorption coefficient and inflection point of the opacity law are fixed at $2.5 \times 10^3 cm^{-1}$ and 9.7 microns. It is clear that the polarization data require that the opacity law be skewed toward long wavelengths. The range of Trapezium dust temperatures is not significantly different from 250°K. We can conclude that the empirical opacity law is supported by the polarization data, a result which is independent of any assumptions about the Trapezium emission.

Grain Shape and Alignment

The success of the linear dichroism model in explaining the wavelength dependence of the polarization gives strong support to the original suggestion of Dyck et al. (1973) that the polarization is produced by absorption in partially aligned dust particles. It remains

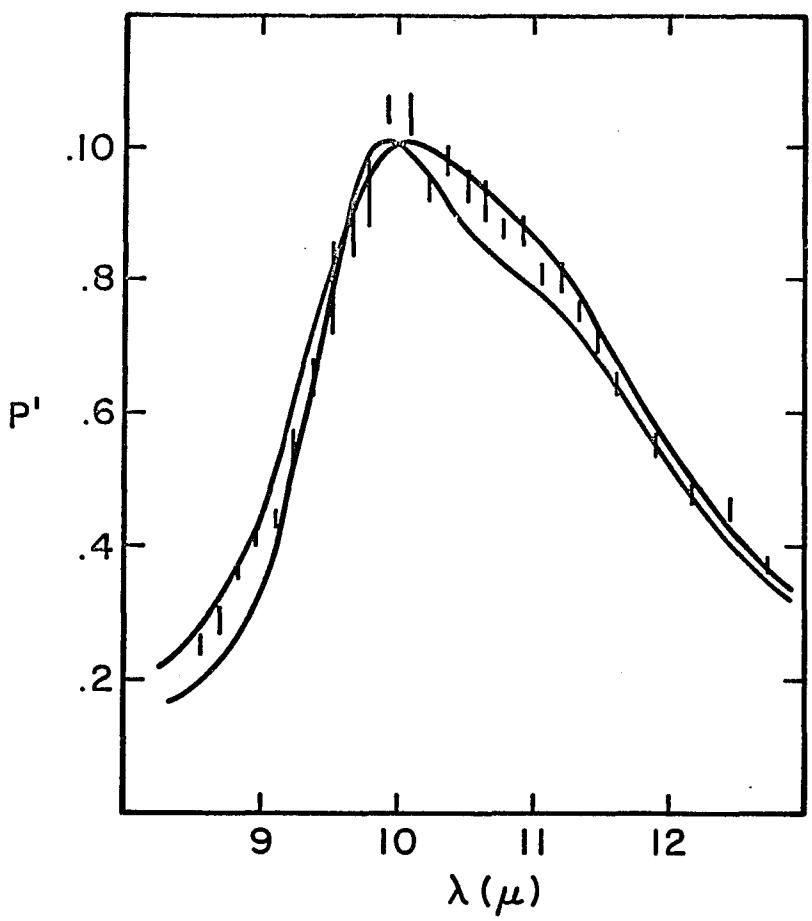

Fig.. 3.4. Approximate Range of Polarization Curves Allowed by the Observational Errors.

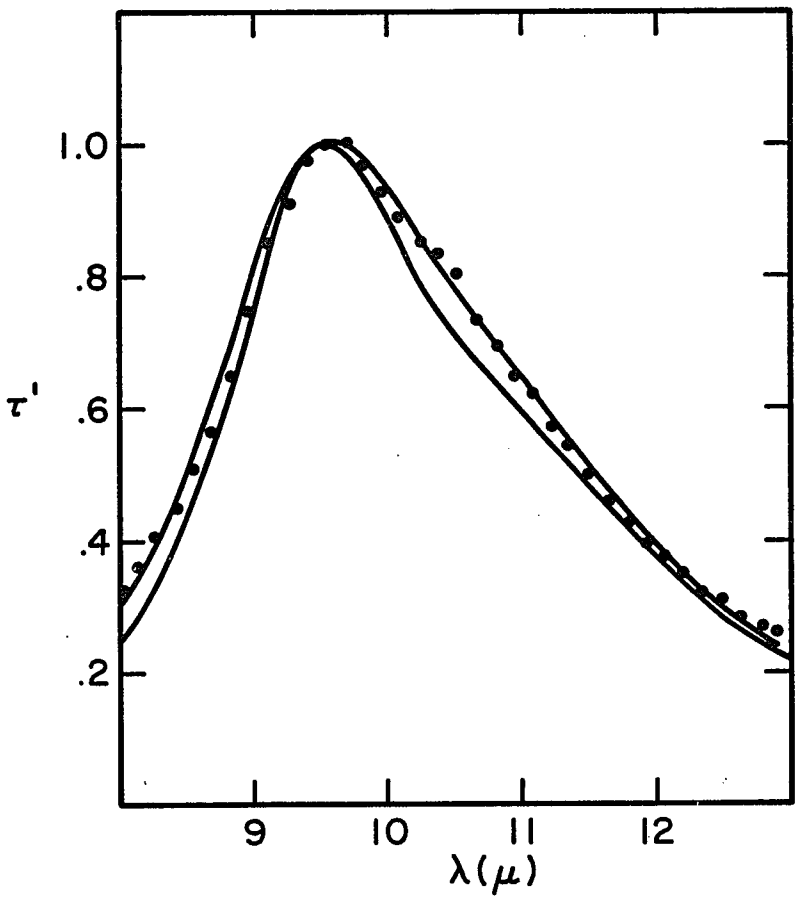

Fig. 3.5. Comparison of the Range of Silicate Opacity Laws Allowed by the Polarization Data with the Opacity Law Generated by GFMCS.

to examine the requirements which are placed upon the shape of the grains and the efficiency of the alignment mechanism in order to produce the observed polarization. With regard to possible alignment mechanisms, the grains responsible for the 10 micron polarization are located in a much more restrictive environment than that of the normal interstellar medium. DB consider the likely mechanisms within this context and conclude that because of the large visual attenuation of the dust cloud and the direction of the polarization, the large scale alignment which they observe can only be explained easily by the presence of a well-ordered magnetic field. They then proceed on the assumption that the alignment is by the Davis-Greenstein (1951) mechanism (DG) and find limits on the shape of the grains and the required magnetic field strength. Martin (1975) expands on this discussion and also sets limits on the inclination of the alignment direction with respect to the plane of the sky.

The dichroic absorption process has been shown to represent the data accurately. However, the polarization observations presented here do not add materially to the observational evidence upon which the previous estimates of grain shape and alignment depend. Elimination of the absorption coefficient still leaves the shape (oblate or prolate), axial ratio, and background refractive index of the grains as free parameters in the determination of S. In addition, the observed value of P/τ depends upon the degree of alignment and inclination of the alignment direction with respect to the plane of the sky. However, it seems worthwhile to reconsider the assumptions contained in the previous work

and to examine the results in light of the radiative models which are now available.

Limits have been set on the shape of the grains by asking what the minimum axial ratio must be in order to produce the observed polarization. The answer is derived by setting the alignment parameter equal to its formal maximum value, $Q_A = 1.0$ for oblate grains or $Q_A = -0.5$ for prolate grains, and then adjusting S until it is equal to the minimum possible value of P/τ. This method produces a definite lower limit on the axial ratio of the grains. However, it is excessively conservative.

In order to achieve alignment, two things must occur. First, some mechanism must provide a preferred direction for the grain's angular momentum which, in the case of magnetic alignment, is through paramagnetic relaxation that damps the grain's rotation about those space axes which are not parallel to the field direction. Second, it is necessary for a correlation of the direction of the body axes of the grain and the direction of the angular momentum to exist. For instance, the angular momentum of a cloud of spherical grains could be perfectly aligned; however, since the moment of inertia of a sphere has no preferred direction, the body axes of the spheres could never be aligned. In general, the alignment of the angular momentum and the alignment of the grain's symmetry axes are coupled. However, Jones and Spitzer (1967) have shown that the coupling is not strong for most grain shapes and that the problem can be simplified in order to uncouple the two parts of the alignment process. Subsequently, Purcell and Spitzer

(1971) examined the errors introduced by the simplifying assumptions and found that for grains with axial ratios larger than 5, the uncoupled equations introduce errors of less than 25%. In its uncoupled form, the alignment parameter is given by

$$Q_A = Q_J Q_X \cdot \qquad (3.15)$$

Q_J is the alignment of the angular momentum of the grains with respect to the magnetic field and Q_X is the correlation of the grain's symmetry axis with the direction of the angular momentum. Q_X is dependent only on the shape of the grain,

$$Q_X = 1.5\, q(\gamma - 1) \qquad (3.16)$$

$q(X)$ is a function given by Jones and Spitzer (1967) and γ is the ratio of the moment of inertia about the grain's symmetry axis to the moment of inertia about a transverse axis,

$$\gamma = 0.5[(b/a)^2 + 1] \qquad (3.17)$$

a is the length of the long axis and b is the length of the short axis.

For spheroidal grains of a given axial ratio, R, and shape, the maximum value of $P/\tau)_\lambda^{max}$ is given by

$$P/\tau)_\lambda^{max} = \frac{Q_X(R)S(\lambda,R)}{2}, \quad Q_J = 1 \qquad (3.18)$$

This product is displayed in Fig. 3.6 for representative values of the background index of refraction. The value of γ for oblate grains cannot be larger than 0.5, which means that Q_X will not be larger than 0.144. Using $m_o = 1.7$, $P/\tau)_\lambda^{max} = 0.095$. For prolate spheroids, Q_X

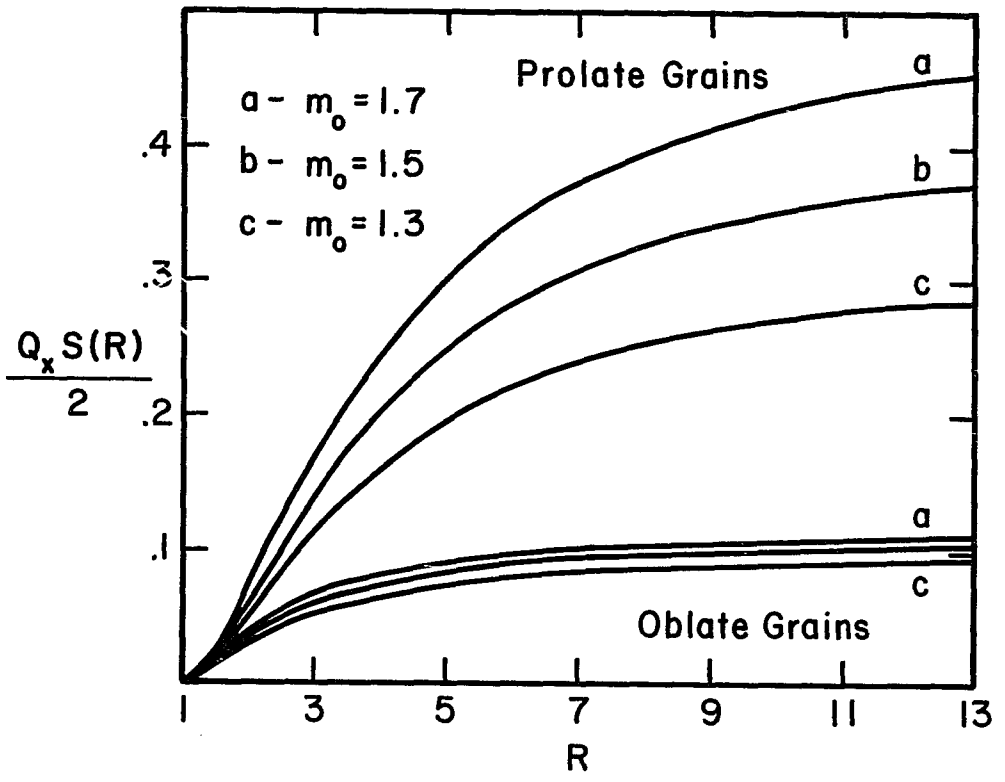

Fig. 3.6. Polarizing Efficiency of Ellipsoidal Grains Spinning about Their Symmetry Axes.

approaches its maximum value of 0.5 for R > 10. $P/\tau)_{\lambda}^{max}$ is then 0.45.

The observed value of P/τ depends upon how τ is determined. The unknown level of the underlying continuum, a classical problem of visual spectroscopy, is the uncertainty which enters the problem. GFMCS have attempted to find the range of possible values of τ by modeling the continuum with a blackbody (Model I) and also an optically thin, Trapezium-like source (Model II). Model I yields a central optical depth of 1.7 and Model II requires a larger value of 3.3. Scaling the optical depth with the resonance model opacity law, we have, $P/\tau)_{11\mu} = 0.101$ and 0.052 for Model I and II respectively. If Model I applies, oblate grains cannot produce the required polarization. If $Q_J = 1$, then the prolate grains must have R > 2.7 or, if R > 10, the alignment of the angular momentum must be such that $Q_J > 0.22$. Model II reduces the constraints considerably. Both oblate and prolate particles are formally allowed, with R > 2.5 or 1.8, respectively. For sufficiently large axial ratios, we find that $Q_J > 0.55$ for oblate grains and $Q_J > 0.12$ for prolate grains. Despite the larger polarizing efficiency of oblate grains, the relative ease of aligning prolate grains dominates in choosing the most likely particle shape.

Various alignment mechanisms will be considered in the next chapter. We have seen that the minimum alignment required to account for the BN polarization is $Q_J = 0.12$. This value will be used to study the conditions in the dark clouds which are necessary in order to produce the alignment. A new mechanism which may change the shape limits

for the BN grains is due to Purcell (1975). He has proposed a modification to the DG theory which he calls "pinwheeling." Through a number of possible schemes, he believes that interstellar grains can behave like tiny anemometers or pinwheels. The grains are able to achieve much higher spin rates than expected from thermal equilibrium, which significantly improves the efficiency of paramagnetic relaxation. The pinwheeling mechanism can produce complete alignment of the grain's body axes without difficulty. However, the theory of pinwheeling has not developed to the point that the grain's shape can be separated from the resulting alignment. In fact, prolate grains may spin around their symmetry axis. In order to produce the observed polarization, we can only require that $R > 1.5$ for Model I or $R > 1.1$ for Model II. Purcell poses a modest conflict in noting that the stresses resulting from the high rotation rates of pinwheeling grains might destroy conglomerate particles such as those suggested by the small 10 micron absorption coefficient of the grain material.

CHAPTER 4

OBSERVATIONS OF ADDITIONAL COMPACT SOURCES

The BN observations have shown that 10 micron polarimetry can provide considerable information about the composition, shape, and environment of the silicate grains. These results are important in understanding the Orion region; however, their ultimate value depends on establishing their applicability to the general class of compact infrared sources. This can only be established by observations of other compact sources.

Observations

In order to survey the polarization properties of a number of compact sources cadidate objects were selected from the group which have been observed spectroscopically by Merrill and Soifer (1974), GFMCS (1975), and Gillett and Capps (in preparation). The brightest sources were chosen from this group and as wide a range of apparent optical depths as practical were included. Minimal selectivity was justified by the survey nature of the observations and necessitated by the sensitivity limits of the equipment. An unexpected fallacy has been revealed by the recent work by Soifer et al. (in preparation). They have shown that one of the candidate objects, UOA 19, has variable flux and width of the silicate band. This

distinction sets it apart from the general group of compact sources and may make the interpretation of its observations questionable.

The observations were carried out at KPNO with the 1.3 meter telescope during October and November 1973 and September 1975. Data were also obtained with the 2.1 meter telescope during October 1975 and June 1976. The data from 1973 were obtained with an Infrared Laboratories bolometer system. The closed cycle cooler system replaced the bolometer in 1975 and the observations from June 1976 were produced by an uplooking InSb system. A wire grid polarizer was used in all cases.

The observational results are collected in Table 4.1. The effective wavelengths and passbands of the filters have been described previously in Table 2.1. The 10.5 micron points were obtained with the filter wheel set at that wavelength, giving a bandwidth of .2μ. The majority of the observations used a 16 $\hat{n}$ field aperture and a 30 $\hat{n}$ chopper throw. The exceptions are W33A, and the 10.5 micron measurement of NGC 7538 IRS 1, which were measured with a 7 $\hat{n}$ and 10.5 $\hat{n}$ field aperture, respectively. The observations of CRL 2688 are included as an example of a source whose polarization is produced by scattering (Ney et al. 1975). The errors in the position angle are not included in order to simplify the table. These errors are directly related to the error in the magnitude of the polarization. For a 3σ result, the position angle error is less

Table 4.1. Observations of Compact Sources

Object	3.5μ	8.4μ	10.5μ	11.5μ	12.6μ
W33A	.124±.004 63°	--	--	--	--
UOA 19	.015±.006 162°	.012±.008 180°	--	.019±.006 99°	--
W51 IRS2	--	.016±.029 -	--	.021±.004 160°	--
K3-50	--	--	.006±.023 -	.013±.008 59°	--
UOA 27	.052±.003 169°	.023±.007 167°	.050±.009 163°	.030±.003 164°	.026±.003 168°
NGC 7538 IRS1	.028±.009 146°	.028±.013 149°	.018±.011 74°	.036±.008 150°	--
W3 IRS5	.084±.022 70°	.022±.007 88°	.039±.056 -	.034±.017 91°	.025±.005 94°
BN	.083±.003 116°	--	.122±.004 119°	.063±.007 114°	--
CRL 2688	.200±.049 137°	--	*006±.003 148° *Δλ = 5μ	--	--

than 10°. In the case of uncertainties larger than 20°, the position angle is deleted. The relationship of σ_p and σ_θ is discussed in Appendix A.

W3 IRS5 and especially UOA 27 show the characteristic increase in polarization near the silicate band and also at 3.5 microns which indicates dichroic absorption. NGC 7538 IRS1 has a possible large position angle rotation at 10.5 microns. Unfortunately, this measurement was obtained with a smaller field size than the others and may indicate that other sources contaminate the flux. This point requires observational confirmation since it may indicate that the absorption coefficient of the grains is much larger than in BN. The measurement of W33A was made with the InSb detector system. In this case, scattering cannot be eliminated as the source of the large 3.5 micron polarization. The huge silicate and ice optical depths, $\tau_{9.6} \geq 7$ and $\tau_{3.05} > 9$ (Gillett and Capps (in preparation), might allow a significant scattering optical depth also. Extrapolation to longer wavelengths is not particularly reliable; however, on the basis of BN's wavelength dependence, W33A could reach P = .2 at 10 microns if dichroic absorption produces the polarization.

Average Source Characteristics

The most striking result of the observations is that at 11.5 microns BN is significantly more polarized than any of the other sources. The dichotomy is even more apparent in the values

of P/τ. Optical depths based on model fitting of the spectra are not available for all of the sources. Therefore, in order to have an estimate of the optical depth, a minimum value was established by fitting a linear continum between the long and short wavelength peaks of the 10 micron spectrum. The required central optical depth was scaled by GFMCS' capacity law to give a minimum optical depth, τ_{min}, at 11.5 microns.

This procedure is roughly equivalent to assuming that the underlying continuum is a blackbody (GFMCS' Model I, 1975). If the spectrum were actually self-absorbed, the central optical depth would be underestimated by the amount necessary to attenuate the silicate emission. Examination of the GFMCS models shows that the difference in the central optical depths of Model I and Model II is reasonably constant at $\Delta\tau = 1.7$. The difference at 11.5 microns would be $\Delta\tau_{11.5} = .85$. If all of the sources are self absorbed, then the optical depth will be underestimated by an additive value of $\Delta\tau_{11.5} = .85$. If some of the sources are self-absorbed and others are black bodies, the optical depth estimate will introduce scatter in P/τ. The range of values can be approximated by dividing the following analysis into two cases,

$$\tau)_I = \tau_{min}$$
$$\tau)_{II} = \tau_{min} + .85 \qquad (4.1)$$

For each of the sources, τ_{min}, $P/\tau)_I$ and $P/\tau)_{II}$ are listed in Table 4.2. The uncertainties reflect the statistical errors in P only.

Armed with the thought that a statistical discussion which is based upon only seven data points may be misleading, we can examine the probable explanations for the apparent uniqueness of BN. Assuming the polarization at 11.5 microns is produced by dichroic absorption, the ratio of P and τ is specified by Eq. 2.3. The fact that this ratio is observed to be generally much smaller than for BN must be due to a deficiency in one or more of its three component factors, S, the grain optical properties, $Cos^2\Psi$, the alignment direction, and Q_A, the degree of alignment.

It is unlikely that the grains are incapable of producing large polarizations. We have seen that, unless the grains are nearly spherical, they can produce the polarization observed in BN. The only effective way to extinguish their polarizing efficiency is to reduce the absorption coefficient of the material. The BN grains are already within a factor of 1.5 of the lower limit on the absorption coefficient, which does not leave much room for further reductions. The dependence of S on the axial ratio (Fig. 3.6) shows that the transition between weak and strong polarizers occurs over a small range of R. The existence of some polarization in most of the sources requires that the grains are nonspherical and suggests that they are intrinsically strong polarizers.

Table 4.2. Source Characteristics

Object	τ_{min}	$P/\tau)_I$	$P/\tau)_{II}$
W33A	3.5	.03*	.024*
UOA 19	1.3	.015±.004	.009±.003
W51 IRS2	0.4	.060±.011	.019±.004
K3-50	0.4	.037±.021	.012±.007
UOA 27	1.0	.030±.003	.016±.002
NGC 7538 IRS1	1.9	.019±.004	.013±.003
W3 IRS5	2.2	.016±.007	.012±.006
BN	0.6	.105±.011	.043±.005

* P estimated from wavelength dependence of BN

Presumably, the alignment direction depends upon either some general property of the galaxy, such as the magnetic field direction, or the local conditions within each source. Table 4.3 lists the galactic coordinates (l,b) and position angle of the galactic plane α for the measured sources. If the alignment direction were the direction of the galactic magnetic field, ψ would be approximately equal to the galactic longitude, l, of the source. In this case, a

Table 4.3. Source Position Data

Object	l°	b°	α°
W33A	12	-1	27
UOA 19	24	-1	25
W51 IRS2	48	+1	32
K3-50	68	+1	32
UOA 27	76	-2	38
NGC 7538 IRS1	112	+2	68
W3 IRS5	132	+2	68
BN	208	-18	72

correlation between P/τ and $\cos^2 l$ should exist. Fig. 4.1 compares these two quantities. The open circle is UOA 19 and the upper limit is W33A. Without the BN point, there would be no obvious relation between the two quantities; however, the BN point admits the possibility of an envelope relationship, as indicated by the dashed lines. It would follow that the alignment is due to the galactic field, with a variable degree of alignment which fills the envelope below the maximum value. This notion, or any other alignment mechanism which uses a general property of the galaxy, should preferentially align the grains in the galactic plane or possibly perpendicular to it. Averaging the differences between the position angle of the polarization and the local position angle of the galactic plane, we have $(\theta-\alpha) = 25°$, with the standard deviation of a single observation equal to 48°. The distribution of position angles is essentially random with respect to the galactic plane. This test indicates that the alignment direction is random and that local conditions control the alignment of the grains.

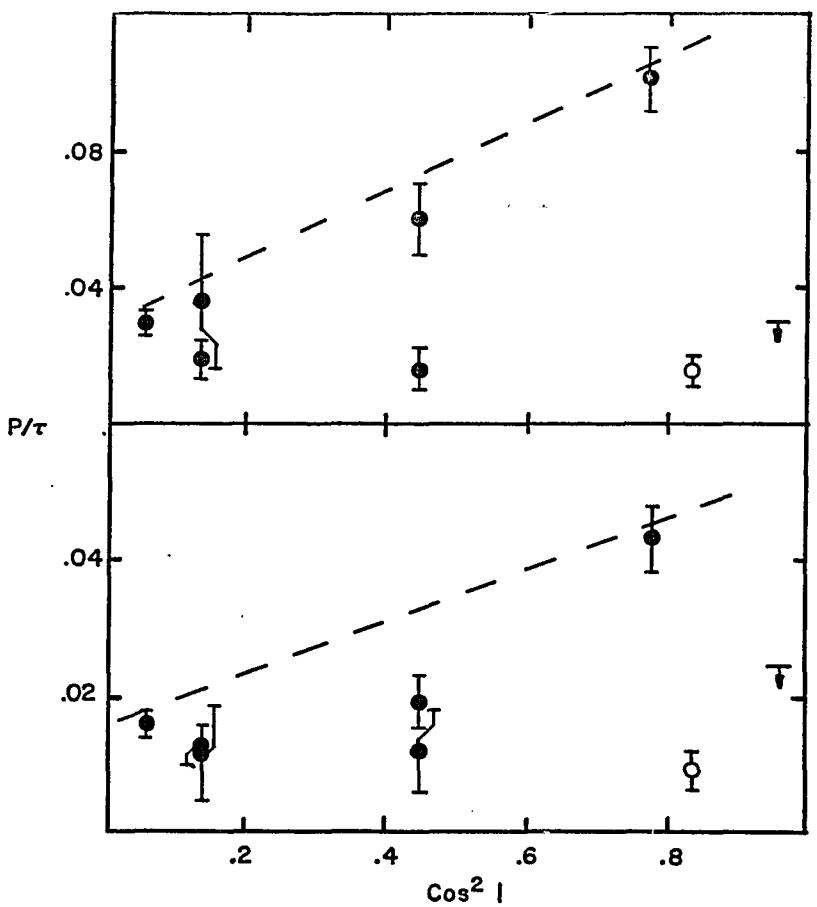

. Fig. 4.1. Distribution of P/τ with Galactic Longitude.

Local properties of the sources apparently produce the grain alignment; however, we shall see that a random alignment direction, by itself, cannot produce the observed distribution of P/τ values. The expected value of P/τ should be no less than

$$\langle P/\tau \rangle \geq \langle \cos^2\psi \rangle \ (P/\tau)_{BN} \tag{4.2}$$

Averaged over solid angle gives $\langle \cos^2\psi \rangle = .666$ and

$$\langle P/\tau \rangle_I \geq .074 \pm .007 \tag{4.3}$$

$$\langle P/\tau \rangle_{II} \geq .029 \pm .003$$

Averaging over all the sources except UOA 19 and W33A, we have

$$(P/\tau)_I = .046 \pm .015 \tag{4.4}$$

$$(P/\tau)_{II} = .019 \pm .005.$$

The expected and observed average values of (P/τ) do not agree for either Case I or II. The probability that the same degree of alignment occurs in both BN and the average compact source is very small. For both Case I and Case II, the analysis shows that

$$Q_A > 0.6(Q_A)_{BN} \tag{4.5}$$

Recalling the discussion of the BN observations, it was found that

$$Q_J)_{BN} \geq 0.12 \tag{4.6}$$

which leads to

$$Q_J > 0.07 \qquad (4.7)$$

for the average compact source, assuming the grains are similar and that dichroic absorption produces the polarization. The apparent distinction of BN is that the alignment mechanism operates most efficiently there.

Alignment Mechanisms

The dichroic absorption process requires that the grains present a net absorption asymmetry in the line of sight to the source. This fact can be used to rule out alignment mechanisms which produce radial alignment with respect to the central source. Although there may be others, two such processes are photon angular momentum exchange (Harwitt, 1970), which produces radial alignment of the grain's angular momentum, and radiation driven streaming (Purcell, 1969), which produces a correlation of the grain's minimum cross section with the radial direction. This conclusion has also been reached by Carrasco, Strom, and Strom (1973) from visual polarization measurements of stars in the Oph dark cloud. They found that even the brightest stars, which are expected to be the alignment sources in the case of the previously mentioned mechanisms, are polarized. In the case of BN, the Trapezium stars might be the alignment center; however, DB point out that this cannot be the case because the direction of polarization is approximately 45° to the line joining the Trapezium and BN.

In the previous chapter, it was shown that perfectly aligned ($Q_J = 1$), spinning prolate grains could produce $P/\tau)_{11} = .45$. Therefore, in order to produce the observed polarization of BN, we require a minimum optical depth due to aligned grains of $\tau)_{11} = .15$ or $\tau_{9.6} = .30$. More realistic estimates of Q_J, such as those of Purcell and Spitzer (1971), would require that the optical depth of aligned grains be $\tau_{9.6} > 1.2$. Apparently a significant fraction of the grains in the line of sight are involved in producing the polarization. Therefore, the alignment mechanism must involve a general property of the cloud. The candidate cloud properties which could lead to significant grain alignment are a strong imbedded magnetic field and large scale streaming which would produce alignment through the mechanism of Gold (1952).

Let us first investigate the magnetic field strengths which might occur in the compact sources. Larson (1973) discusses the evolution of a cloud contracting in a magnetic field. At low densities, the level of ionization produced by cosmic rays is sufficient to carry the magnetic field along with the gas during the contraction. The field will remain "frozen in" until the gas density reaches a level where cosmic ray screening prevents ionization of the interior of the cloud. Oppenheimer and Delgarno (1974) investigate the ionization of dense interstellar clouds and find that the field will remain frozen until $n > 10^6 cm^{-3}$. The density estimates of GFMCS (1975) are $n\ (H_2) > 10^5 cm^{-2}$, which suggests that the field is not diffusing rapidly out of the compact sources. As long as the field is frozen

in, $B \alpha \rho^{2/3}$ as the cloud contracts. Therefore, at a density of n (H_2) = 10^5, we expect the galactic magnetic field to be compressed to a value of $B = 1.4 \times 10^{-3}$ gauss.

Spitzer (1968) has shown that in order for a non-rotating cloud to contract spherically in the presence of a uniform, frozen in, magnetic field, its mass must be greater than a critical mass,

$$M_c = .024\ B^3/(G^{3/2}\ \rho^2) \qquad (4.8)$$

where $G = 6.67 \times 10^{-8}$ (dynes $cm^2 g^{-1}$) is the gravitational constant, B is the magnetic field strength (gauss) and ρ is the mass density (g cm^{-3}). For a galactic field of 3×10^{-6} gauss and n(H) = 20, $M_c = 1.2 \times 10^4$ M. Mass estimates for the molecular clouds associated with the sources studied by GFMCS are $M_{tot} \gtrsim 10^5$ M, which are compatible with contraction initiated in the ambient galactic environment.

Spitzer points out that the magnetic field does not impede collapse along the field lines. This allows the density to grow without increasing B until Mc is reduced to the point where collapse across the magnetic field is possible for masses which are smaller than Mc. Therefore, strong magnetic fields should be a general result of gravitational collapse.

The magnetic field is constrained within the cloud by the drag forces of the neutral gas on the ions. Once compressed, the field will diffuse through the neutral gas at a velocity determined by the field strength and the collision rate of ions and neutrals. For the

case of straight, parallel field lines, Spitzer (1968) gives the diffusion velocity as

$$V_D = \frac{\nabla B^2}{8\pi\, n_i\, m\, \langle\sigma V_T\rangle} \tag{4.9}$$

where B is the magnetic field strength, n_i is the ion density, n, m, and $\langle\sigma V_T\rangle$ are the density, mass, and ion collision rate constant of the neutral particles. Presuming that the neutrals are predominantly H_2 molecules, and that the average density is $n_{H_2} = 10^4$ cm^{-3}. Oppenheimer and Delgarno (1974) give $n_i = 4 \times 10^{-3}$ cm^{-3}. $\langle\sigma V_T\rangle$ 2×10^{-9} cm^3/sec is given by Watson (1974) for dark cloud conditions. Therefore, perpendicular to the field,

$$V_D = 1.5 \times 10^{29}\ \frac{\Delta B^2}{\Delta r}\ \text{cm s}^{-1} \tag{4.10}$$

Spitzer shows that for a uniform field and density distribution, the time required for the field to diffuse out of the cloud is

$$t_D = 5.3 \times 10^{13}\ n_i/n \text{ years.} \tag{4.11}$$

We have $n_i/n = 4 \times 10^{-7}$ for $n = 10^4$, which gives

$$t_D = 2 \times 10^7 \text{ years.} \tag{4.12}$$

If the field gradient is as large as 10^{-3} g/pc, the magnetic field would diffuse out of a one parsec region in 2×10^6 years.

We can consider the magnetic field to be reasonably constant if the free fall time of the material is less than the diffusion time. Following Nakano and Tademaru (1972),

$$t_f \approx \left(\frac{\delta\pi}{3} G\rho\right)^{-\frac{1}{2}} = 2.4 \times 10^5 \text{ years}, \qquad (4.13)$$

$$n(H_2) = 10^4 \text{cm}^{-3}$$

The magnetic field is, therefore, essentially constant during the lifetime of the cloud. However, if significant grain alignment is to occur, there must also be sufficient time for substantial modification of the grain's angular momentum. Purcell and Spitzer (1971) demonstrate that the time for rotational damping due to gas friction is never greater than the time for the grain to be struck by its own mass of gas atoms. This time is

$$t_m = \frac{4M}{A\langle v\rangle\rho} \qquad (4.14)$$

where M is the mass, A is the total surface area of the grain, $\langle v\rangle$ and ρ are the average velocity and density of the gas. For uniform spherical grains,

$$t_m = \frac{4}{3}\frac{r\rho_g}{\langle v\rangle\rho} \qquad (4.15)$$

r and ρ_g are the radius and density of the grain. For a gas temperature, T = 30°K, the average velocity of H_2 molecules is $\langle v\rangle = 6 \times 10^4$ cm/sec. We take $r = 10^{-5}$ cm and $\rho_g = 3$ g cm^{-3} and $\rho = 3.2 \times 10^{-20}$ g/cm^{-3}. The rotational damping time is then

$$t_m = 6 \times 10^2 \text{ years}. \qquad (4.16)$$

During the lifetime of the cloud, the magnetic field is reasonably constant and the grain rotation can be changed many times by gas friction. The stage is, therefore, set for grain alignment through interactions of the grains, gas, and magnetic field.

The standard mechanism which is thought to produce magnetic alignment in the interstellar medium is the DG process. It has received several iterations in the literature and its success is reviewed by Aannestad and Purcell (1971). In the formulation of Purcell and Spitzer (1971), the angular momentum alignment is given by

$$Q_J = \frac{3}{2} \; q\left[\frac{\delta}{1+\delta} \quad \left(\frac{T_g - T_e}{T_e}\right)\right] \tag{4.17}$$

Where q(x) is a distribution function derived by Jones and Spitzer (1967), T_g is the grain temperature, and T_e is the equilibrium rotational temperature of the grain in the absence of any fields. The ratio of aligning magnetic torques to randomizing torques is δ, which is also equal to the ratio of the magnetic and gas damping times. For significant alignment, we expect $\delta > 1$.

In order for alignment to occur, the grain temperature and the effective rotation temperature must be different. The lower limit on the effective temperature is the gas temperature because, in the absence of other torques, the rotation of the grain would be in thermal equilibrium with the gas. If this were the case in compact sources, we would expect $0.5 < T_g/T_e < 2$ (Larson 1973; Goldreich and Kwan 1974),

which would make DG alignment difficult. However, there are many ways to increase T_e, such as cosmic ray impacts (Salpeter and Wickramasinghe, 1969), reaction forces of H_2 formation (Purcell and Spitzer 1971), and variations in the grain's accommodation coefficient (Purcell, 1975). Purcell (1975) suggests that $T_g/T_e = 0$ is a good estimate of the ratio of the grain and effective temperatures.

Using this estimate,

$$Q_J = \frac{3}{2} \quad q\left(\frac{\delta}{1+\delta}\right) \tag{4.18}$$

For the average compact source, the lower limit is $Q_J)_{ave} = 0.07$ and for $Q_J)_{BN} = 0.12$. The related values of δ are $\delta)_{ave} = 0.43$ and $\delta)_{BN} = 0.79$. In the formulation of Purcell and Spitzer (1971),

$$\delta = C \frac{K B^2}{\langle v \rangle \rho V^{1/3}} \tag{4.19}$$

where C is a shape factor, B is the magnetic field strength, $\langle v \rangle$ and δ are the average speed and density of the gas, V is the grain volume, and $K = X''/\omega$ is the ratio of the magnetic susceptibility and angular velocity of the grains.

The limit on δ requires a grain axial ratio of 7, which gives $C = .3$. Jones and Spitzer (1967) find that $K = 2 \times 10^{-12}/T_g$ sec for normal paramagnetism at the frequencies of interest. For a representative grain size, we take $V^{\frac{1}{3}} = 10^{-5}$ cm. The regions we have considered have $n(H_2) = 10^4$. Microwave observations indicate that the gas temperature is between 30°K and 100°K (Zuckerman and Palmer 1974).

Infrared observations of compact source clouds indicate a grain temperature of 60°K (Harper and Low, 1971). Goldreich and Kwan (1974) argue that the total CO flux requires that the grains absorb radiation from the central source and heat the gas. They conclude that the grains must be hotter than the gas and at the temperatures indicated by the 100 micron observations. Prior to the formation of a central "star", the grains may have been much colder. We will use $T_g = 50°K$. The resulting minimum magnetic fields are

$$B)_{ave} = 8.7 \times 10^{-4} \text{ gauss} \qquad (4.20)$$

$$B)_{BN} = 1.2 \times 10^{-3} \text{ gauss.}$$

B is not sensitive to the various parameters which enter the calculation because of the square root dependence. Therefore, these values of B are representative of the required aligning field.

We have seen that it is possible to produce magnetic fields of this size in the compact sources. However, the conditions must be ideal in order to produce the observed polarization. The standard escape from this situation is to invoke superparamagnetic absorption. Aannestad and Purcell (1971) suggest that a 1% concentration of small iron or magnetite inclusions in the grain could increase K by several orders of magnitude. The required magnetic field could be smaller by a factor of ten.

Purcell (1975) has proposed that some of the processes which affect the grain's angular momentum may not be random. In particular,

if the accommodation coefficient (gas sticking probability) or the location of the sites of H_2 formation have permanent irregularities, the grain's angular momentum exchange with the gas will not be random. The systematic torques which result will spin-up the grain to supra-thermal rates about either its long or short grain axis. This is the basis of Purcell's pinwheeling mechanism.

The pinwheeling grains are aligned by the same magnetic torque which produces DG alignment. The advantage of pinwheeling is that the time during which the alignment is produced may be much longer than the rotation damping time, t_m. If the grain irregularities never change, the alignment can build up during the free fall time of the cloud. The required field is thus reduced by $(t_m/t_f)^{\frac{1}{2}} = 5 \times 10^{-2}$. On the other hand, if the irregularities are modified by grain-gas collisions or frozen on surface layers, the systematic torques may last for times which are much less than t_m. In this case, the DG theory describes the alignment, with $T_g/T_e = 0$. As long as the grain and gas temperatures are different, Purcell sees no way to avoid systematic torques on real grains. Unfortunately, the time scale over which they operate is very uncertain.

The conditions in the compact source clouds may allow an alternative to the various DG related alignment mechanisms. The previous discussion of the diffusion of the magnetic field out of the cloud gives a diffusion velocity of 6×10^4 cm sec^{-1} with a field gradient of 10^{-3} gauss pc^{-1} . The diffusion velocity will therefore

be approximately equal to the random thermal velocity of the gas. If the grains carry sufficient excess charge, they will be locked to the field like the ions. It follows that the differential streaming of the grains and neutral gas will partially align the grains (Gold, 1952). Purcell (1969) finds that for a ratio of stream to random velocity of 1, $Q_J = .12$ for most grain shapes.

Aside from the question of the grain charge, the streaming process depends upon magnetic fields which are as large as those required by ordinary DG alignment. In addition, if the effective rotation temperature of the grains is much larger than the gas temperature, streaming motions of 1 km/sec will not produce sufficient alignment. The angular momentum exchange which does occur due to streaming adds constructively to the DG process because the streaming direction will be transverse to the magnetic field. Diffusion streaming becomes one of the processes which increases the effective rotation temperature of the grains.

In the event that the grain and gas temperatures are equal and higher than 25°K, most of the nonthermal spin-up mechanisms are inoperative. H_2 formation is inhibited and, since no energy exchange occurs between the grains and the gas, variations in the accommodation coefficient have no effect. In this situation, especially deep in the cloud, diffusion streaming could be an important source of alignment if the grains can carry excess charge at densities greater than $n = 10^5$ cm^{-3}.

In general, the viable alignment schemes require magnetic fields in excess of those found in the interstellar medium. However, without additional observational constraints, the range of acceptable values remain uncertain by several orders of magnitude.

Galactic Center Sources

The infrared sources associated with the nucleus of our galaxy are not necessarily related to the compact sources. However, they have many spectroscopic properties which are similar. Of particular interest is the silicate absorption feature which appears in all of the 10 micron sources and which is found to vary in depth between individual sources (Gillett and Capps, in preparation). Following an unsuccessful measurement by Low et al. (1969), Dyck, Capps, and Beichman (1974) detected 10 micron polarization from these sources. Using the same equipment and techniques which were used here, Capps and Knacke (in press and in preparation), obtained filter wheel resolution measurements of source 1 of Becklin and Neugebauer (1975) and also 11.5 micron measurements of a number of the other sources. The filter wheel data shows the characteristics of dichroic absorption and the P/τ values are within the range of the compact sources. In addition, the correlation of the position angles with any one direction is weak. Capps and Knacke concluded that the polarization is representative of local source conditions and, by analogy with BN-KL, they suggest that the galactic center sources belong to the same group as the other compact sources.

Figure 4.2 is a plot of P/τ versus τ_{min} for the compact sources (filled circles) and also the galactic center sources (open circles). The galactic center data have been analyzed in the same fashion as the compact sources and are listed in Table 4.4. The galactic center sources fall within the range of the compact sources. This is essentially a restatement of the conclusions of Capps and Knacke (in press). The open square is a data point for the nucleus of NGC 1068 which was obtained from the spectroscopic study of Kleinmann, Gillett, and Wright (1976) and the polarimetry of Knacke and Capps (1974). The polarimetry is supplemented with a measurement at 11.5 microns which was obtained as part of this program and which agrees with the previous results. The value of τ_{min} was determined by the same procedure used for the compact sources. Since the underlying continuum is probably different than that of the compact sources, τ_{min} for NGC 1068 may be an underestimate by comparison. Raising τ_{min} by a factor of two would place the NGC 1068 point on top of BN.

This diagram raises a number of questions which can only be resolved with additional observations. The case I picture reveals the possibility that an upper limit on P/τ as a function of τ exists. Should such a relationship be confirmed, it would demonstrate how the average grain alignment varies with optical depth. This would provide additional constraints on cloud models and alignment mechanisms. It is possible that NGC 1068 is polarized by dust. If it is, NGC 1068 is an extreme example of the dichroic absorption process. Higher spectroscopic resolution observations, especially between 7.5 microns and 8 microns would help resolve this important question.

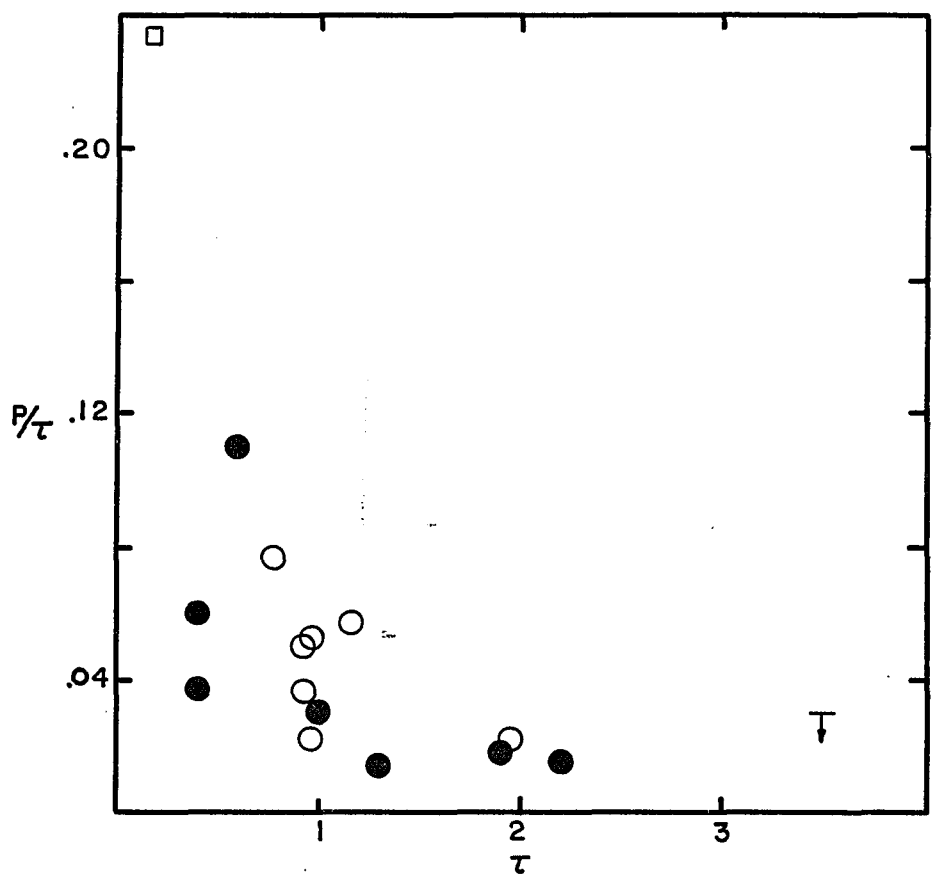

Fig. 4.2. Relation of P/τ and τ_{min} for the Compact Sources and Galactic Center Sources.

a. Case I.

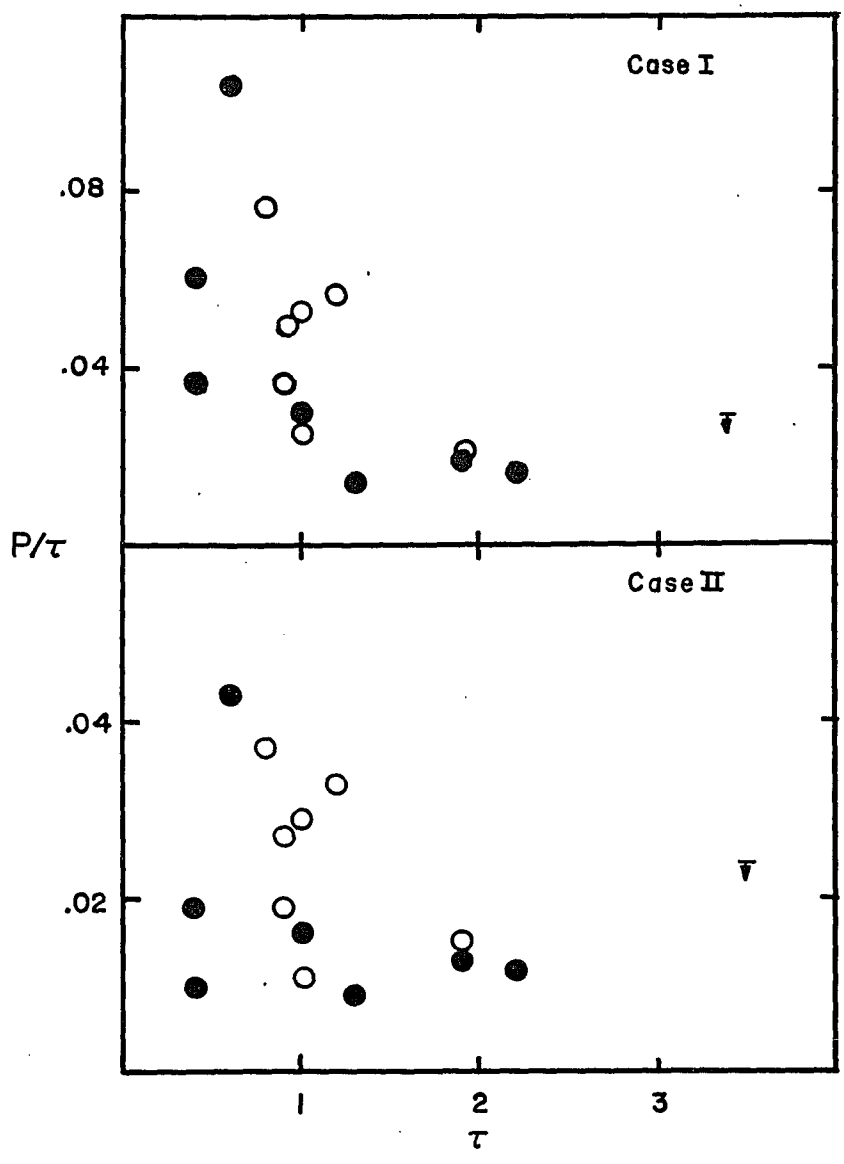

Fig. 4.2, Continued. Relation of P/τ and τ_{min} for the Compact Sources and Galactic Center Sources.

b. Case I and Case II.

Table 4.4. Galactic Center Sources

Source	P(11.5μ)	τ_{min}	$P/\tau)_I$	$P/\tau)_{II}$
1	.059 ± .005	0.8	.076 ± .006	.037 ± .003
2	.035 ± .004	0.9	.037 ± .004	.019 ± .002
3	.041 ± .008	1.9	.021 ± .004	.015 ± .003
5	.024 ± .004	1.0	.025 ± .004	.013 ± .002
8	.066 ± .016	1.2	.057 ± .013	.033 ± .008
9	.052 ± .005	1.0	.054 ± .005	.029 ± .003
10	.047 ± .004	0.9	.051 ± .004	.027 ± .002

CHAPTER 5

CONCLUSIONS

This dissertation has dealt with three general questions. Polarimetric observations of seven compact souces, including detailed observations of BN, have been used to investigate: (1) the polarizing mechanism which operates in the 9.7 micron silicate band, and (2) the distribution of polarization values among a group of sources with a wide range of silicate optical depths. The problem of developing equipment which is capable of obtaining the data has produced a basic understanding of the difficulties of doing 10 micron polarimetry and several alternatives for additional sensitivity improvement.

The observations of BN have demonstrated that dichroic absorption by small particles accounts for the wavelength dependence of polarization in detail. Since the polarizing mechanism has a well defined geometry and is insensitive to the size of the particles, the values of the grain parameters which do control the polarization are easily extracted from the observations. Of particular importance is the strong dependence of the polarizing efficiency of the grains on the value of the silicate absorption coefficient. In the case of the grains surrounding BN, the volume absorption coefficient must be at least a factor of two smaller than typical values of pure silicate materials.

The size and composition of the BN grains is constrained by the lack of detectable polarization between 7.5 and 8 microns. The grains must be much smaller than the wavelength and the metal content must be small enough to keep the imaginary part of the refractive index below 0.02 at 7.5 microns. This fact can be converted into quantitative limits on the metal content when low temperature, infrared, optical constants for absorbing materials become available.

The alignment of the grains in the compact sources apparently depends upon the presence of reasonable uniform magnetic fields which operate on a large fraction of the absorbing grains. The required magnetic field strengths, which are between one and three orders of magnitude stronger than the normal galactic field, can be produced through the gravitational collapse of the cloud material. The range of P/τ values among the observed sources indicates that the field directions of the compact sources are random with respect to axes fixed in the galaxy. In addition, the efficiency of the alignment mechanism varies by at least a factor of two.

The comparison of the polarization properties of the galactic center sources with the compact sources does not reveal any significant differences. Taken as a group, the polarization observations suggest that a relation between the optical depth and the maximum value of Q_A may exist. Verification of this possibility will require observations of a significantly larger number of sources.

The experience gained from using the single channel ten micron polarimeter has revealed a number of potential improvements which can

significantly increase the sensitivity of the system. In view of the probably scientific benefits, continued development of the instrumentation seems highly justified. Aside from NGC 1068, the sensitivity limits have precluded 10 micron observations of extragalactic objects. The possibility of obtaining new observational information about the powerful extragalactic infrared sources provides motivation for a reduction of the current sensitivity barrier.

A complete understanding of the implications that the small silicate absorption coefficient has on the structure and composition of the grains must await a theoretical investigation of the grain optics. However, the value of the volume absorption coefficient and its relationship to other grain properties, such as the strength of the ice band, can be studied empirically for a substantial number of sources. It may be possible to determine observationally how the silicate absorption coefficient is diluted. If it is because of volatile materials which accumulate on the grains in dark clouds, variations in the relative strength of the ice band should accompany variations in the silicate absorption coefficient. In this case, the absorption coefficient of normal interstellar grains is probably similar to pure silicates because the volatile material would be stripped off by the interstellar radiation field. On the other hand, if the dilution is the result of a mixture of both silicate and non-silicate refractory materials which is produced during the formation of the grains, the absorption coefficient should be reasonably constant in the compact sources and the interstellar medium.

We have seen that BN type grains are capable of producing two-thirds of the visual extinction to VI Cyg No. 12. If the interstellar grains are similar to the grains near BN, this fact puts strong constraints on the theories of grain formation. Therefore, the question of variations in grain structure and composition between the normal interstellar medium and dark cloud regions requires additional study. This is an area where improved 10 micron polarimeters can contribute important observational results.

APPENDIX A

DATA REDUCTION

The effect of a perfect linear analyzer on a partially polarized beam is stated by the following formulation (Treanor, 1962),

$$I(\phi) = I_o[1 + P \cos 2(\phi - \theta)] , \tag{A.1}$$

where I_o is the mean intensity, P is the degree of polarization, $(\phi - \theta)$ is the difference in orientation of the beam maximum (θ) and the analyzer axis (ϕ), and $I(\phi)$ is the transmitted intensity. Therefore, it follows that

$$I'(\phi) = I(\phi + 90) = I_o[1 - P \cos 2(\phi - \theta)] \tag{A.2}$$

and

$$\frac{I(\phi) - I'(\phi)}{I(\phi) + I'(\phi)} = P \cos 2(\phi - \theta) . \tag{A.3}$$

Expanding the cosine function yields

$$\frac{I(\phi) - I'(\phi)}{I(\phi) + I'(\phi)} = P \cos 2\theta \cos 2\phi + P \sin 2\theta \sin 2\phi . \tag{A.4}$$

This can be rewritten as

$$f(\phi) = \frac{I(\phi) - I'(\phi)}{I(\phi) + I'(\phi)} = P_x \cos 2\phi + P_y \sin 2\phi , \tag{A.5}$$

where $P_x = P \cos 2\theta$, and $P_y = P \sin 2\theta$ (A.6a,A.6b)

are the normalized linear Stokes parameters of the beam. The goal of the data reduction technique is to solve Eq. (A.5) for P_x and P_y from the measured intensities.

The intensity recorded at each position of the analyzer is a function of the polarization of the beam, the response of the instrument at that analyzer orientation, and the transmission of the atmosphere at the time of measurement. Fluctuations in atmospheric transmission limit the accuracy of the measurements and cannot be compensated for. Since all of the instrumental effects and the stellar intensities are periodic in ϕ, the measured intensities can be expanded in a Fourier series of the form

$$I(\phi) = a_o + \sum_{n=1}^{\infty} a_n \sin n\phi + b_n \cos n\phi \,, \qquad (A.7)$$

where the a_n and b_n are constants. Various terms in this series can be identified with effects we wish to consider. As has been shown by Eq. (A.5), the terms with n=2 are associated with the polarized component of the beam and also instrumental effects having a 2ϕ dependence. Such instrumental effects include polarized response of the detector and possible dichroic effects produced by the optics and filters in the telescope-detector system. The largest instrumental effect is associated with terms having n=1. These effects stem from the non-parallism of the analyzer substrate and transmission variations due to deterioration of the substrate material.

The only terms in Eq. (A.7) which contain astrophysical information are even functions of ϕ, while the principal instrumental effect

is an odd function of ϕ. Therefore, the instrumental effects having n=1 dependence can be removed without affecting the polarization terms by smoothing the data as follows. Define

$$I_1(\phi) = I_1(\phi + 180) = I(\phi) + I(\phi + 180) \qquad (A.8)$$

for each analyzer position. Then $I_1(\phi)$ has the form

$$I_1(\phi) = a_o + \sum_{n=1}^{\infty} a_{2n} \sin 2n\phi + b_{2n} \cos 2n\phi \qquad (A.9)$$

which is a sum of the even terms in Eq. (A.7). The remaining instrumental effects have the same angular dependence as the stellar polarization. Therefore, they can only be evaluated by observing stars with known polarization. In particular, we assume that observations of unpolarized stars must have the form

$$\frac{I_1(\phi)}{I_1'(\phi)} = 1 \, . \qquad (A.10)$$

This condition allows us to remove the remaining instrumental effects.

The mean ratios of orthogonal intensities for the unpolarized stars define the instrumental correction as follows. For each analyzer orientation, the correction is

$$C(\phi) = \frac{1}{N} \sum_{j=1}^{N} \left(\frac{I_1(\phi)}{I_1(\phi)} \right) j \, , \qquad (A.11)$$

where N is the number of unpolarized stars observed. The final corrected orthogonal ratios are then defined as

$$\frac{I_2(\phi)}{I_2'(\phi)} = \frac{1}{C(\phi)} \frac{I_1(\phi)}{I_1'(\phi)} \, . \qquad (A.12)$$

In order to use the corrected orthogonal ratios to evaluate Eq. (A.5), we use the transformation

$$\tanh^{-1}(x) = 1/2 \ln \left(\frac{1 + x}{1 - x}\right), \tag{A.13}$$

where

$$x = \frac{I(\phi) - I'(\phi)}{I(\phi) + I'(\phi)} \tag{A.14}$$

and

$$\frac{1 + x}{1 - x} = \frac{I(\phi)}{I'(\phi)} \quad . \tag{A.15}$$

We then have

$$\frac{I(\phi) - I'(\phi)}{I(\phi) + I'(\phi)} = \tanh \left[1/2 \ln \left(\frac{I(\phi)}{I'(\phi)}\right)\right] . \tag{A.16}$$

Inclusion of the instrumental correction factor leads to the result,

$$f(\phi) = \tanh \left[1/2 \ln \left(\frac{I_1(\phi)}{I_1'(\phi)}\right) - 1/2 \ln C(\phi)\right],$$

$$\phi = 0^\circ, 45^\circ \tag{A.17}$$

or

$$f(\phi) = \left[\frac{I_1(\phi) - I_1'(\phi)}{I_1(\phi) + I_1'(\phi)}\right]_o = \left[\frac{I_1(\phi) - I_1'(\phi)}{I_1(\phi) + I_1'(\phi)}\right]_i$$

$$\phi = 0^\circ, 45^\circ \tag{A.18}$$

From Eq. (A.5), we see that for $\phi = 0^\circ$,

$$f(0) = P_x \tag{A.19}$$

and for $\phi = 45^\circ$,

$$f(45) = P_Y \tag{A.20}$$

Therefore, we define

$$P_{x_o} = \left[\frac{I_1(0) - I_1'(0)}{I_1(0) + I_1'(0)}\right]_o \tag{A.21}$$

for measurement of a program object and

$$P_{x_i} = \left[\frac{I_1(0) - I_1'(0)}{I_1(0) + I_1'(0)}\right]_i \tag{A.22}$$

After averaging over multiple observations, the means and uncertainties are

$$\overline{P}_{x_{o,i}} = \frac{1}{n}\sum_n P_{x_{o,i}}, \quad \sigma^2_{x_{o,i}} = \frac{\sum_n \left(P_{x_{o,i}} - \overline{P}_{x_{o,i}}\right)^2}{n(n-1)} \tag{A.23}$$

and

$$P_x = \overline{P}_{x_o} - \overline{P}_{x_i}, \quad \sigma^2_x = \sigma^2_{x_o} + \sigma^2_{x_i} \tag{A.24}$$

Similar expressions are obtained for P_y by setting $\phi = 45^o$.

The values of P and θ are found from P_x and P_y as follows. From Eqs. (A.6a and A.6b) we have

$$P = \left(P_x^2 + P_y^2\right)^{\frac{1}{2}} \tag{A.25}$$

and

$$\tan 2\theta_o = \frac{P_y}{P_x} \tag{A.26}$$

The errors in P and θ due to errors in P_x and P_y propagate by the relations

$$\sigma_P = 1/2\left(\sigma_x^2 + \sigma_y^2\right)^{\frac{1}{2}} \tag{A.27}$$

and

$$\sigma_\theta \approx 1/2 \tan^{-1}\left(\frac{\sigma_P}{P}\right) \qquad (A.28)$$

The latter relation is a convenient approximation due to Dyck (1968).

Following the established convention, the position angle of polarization is measured from north, through east, with north defined as 0°. Initially, instrumental position angle zero point is arbitrary. Therefore, a correction is established to rotate the position angles into the standard coordinate system. This is accomplished by the method of Gehrels and Teska (1960), which amounts to measuring the instrumental position angle ($\Delta\theta$) of a reference polarizer which is oriented north-south. The resulting position angles values have the form,

$$\theta = \theta_o - \Delta\theta \ . \qquad (A.29)$$

LIST OF REFERENCES

Aannestad, P. A., and E. M. Purcell, Ann. Rev. Astr. and Ap., 11, 309, Eq. 4 (1971).

Aikens, D. K., and B. Jones, Ap. J. 184, 127 (1973).

Angel, R. P. J., and J. D. Landstreet, Ap. J. (Letters) 160, L147 (1970a).

Angel, R. P. J., and J. D. Landstreet, Ap. J. (Letters) 162, L61 (1970b).

Becklin, E. E., and G. Neugebauer, Ap. J. (Letters) 200, L71 (1975).

Capps, R. W., G. V. Coyne, S. J. Coyne, and H. M. Dyck, Ap. J. 184, 173 (1973).

Capps, R. W., and H. M. Dyck, Ap. J. 175, 693 (1972).

Capps, R. W., and R. F. Knacke, Kitt Peak, Tucson, Ap. J. (in press).

Capps, R. W., and R. F. Knacke, Kitt Peak, Tucson (in preparation).

Carrasco, L., S. E. Strom, and K. M. Strom, Ap. J. 182, 95 (1973).

Davis, L., and J. L. Greenstein, Ap. J. 114, 206 (1951).

Day, K. L., Ap. J. (Letters) 92, L15 (1974).

Dyck, H. M., Ph. D. dissertation, Indiana University (1968).

Dyck, H. M., and C. A. Beichman, Ap. J. 194, 57 (1974).

Dyck, H. M., R. W. Capps, and C. A. Beichman, Ap. J. (Letters) 88, L103 (1974).

Dyck, H. M., R. W. Capps, W. J. Forrest, and F. C. Gillett, Ap. J. (letters) 183, L99 (1973).

Dyck, H. M., F. F. Forbes, and S. J. Shawl, Ap. J. 76, 901 (1971).

Dyck, H. M., W. J. Forrest, F. C. Gillett, W. A. Stein, R. D. Gehrz, N. J. Woolf, and S. J. Shawl, Ap. J. 145, 949 (1971).

Frogel, J. A., and S. E. Persson, Ap. J. (to be published).

Gaustad, J. E., Ap. J. 138, 1050 (1963).

Gehrels, T., and T. M. Teska, Pub. A.S.P. 72, 115 (1960).

Gillett, F. C., and R. W. Capps, Kitt Peak, Tucson (in preparation).

Gillett, F. C., and W. J. Forrest, Ap. J. 179, 483 (1973).

Gillett, F. C., W. J. Forrest, K. M. Merrill, R. W. Capps, and B. T. Soifer, Ap. J. 200, 609 (1975).

Gillett, F. C., T. W. Jones, K. M. Merrill, and W. A. Stein, Astron. and Astrophys. 45, 77 (1975).

Gillett, F. C., D. E. Kleinman, E. L. Wright, and R. W. Capps, Ap. J. (Letters) 198, L65 (1975).

Gold, T., Mem. R.A.S. 112, 215 (1952).

Goldreich, P., and J. Kwan, Ap. J. 189, 441 (1974).

Greenberg, J. M., Nebulae and Interstellar Matter, B. M. Middlehurst and L. H. Allen, eds., Univ. of Chicago Press, Chicago (1968).

Harper, D. A., and F. J. Low, Ap. J. (letters) 165, L9 (1971).

Jones, R. V., and L. Spitzer, Ap. J. 147, 943 (1967).

Kemp, J. C., J. Opt. Soc. Am. 59, 950 (1969).

Kemp, J. C.,

Kittell, C., Introduction to Solid State Physics, Wiley and Sons, New York (1971).

Kleinmann, D. E., F. C. Gillett, and E. L. Wright, Ap. J. (in press).

Knacke, R. F., and R. W. Capps, Ap. J. (Letters) 192, L19 (1974).

Larsen, T., IRE Trans. MTT-10, 191 (1962).

Larson, R. B., Ann. Rev. Ast. and Ap. 11, 219 (1973).

Longhurst, R. S., Geometrical and Physical Optics, Longmans, London (1967).

Low, F. J., D. E. Kleinman, F. F. Forbes, and H. H. Auman, Ap. J. (Letters) 157, L97 (1969).

Martin, P. G., Ap. J. 202, 393 (1975).

Merrill, K. M., and B. T. Soifer, Ap. J. (Letters) 189, L27 (1974).

Nakano, T., and E. Tademaru, Ap. J. 173, 87 (1972).

Ney, E. P., K. M. Merrill, E. E. Becklin, G. Neugebauer, and C. G. Wynn-Williams, Ap. J. (Letters) 198, L129 (1975).

Oppenheimer, M., and A. Delgarno, Ap. J. 192, 29 (1974).

Purcell, E. M., Physica 41, 100 (1969).

Purcell, E. M., The Dusty Universe, G. B. Field and A. G. W. Cameron, eds., Watson, N. Y. (1975).

Purcell, E. M., and L. Spitzer, Ap. J. 167, 31 (1971).

Reike, G. H., Ap. J. (Letters) 193, L81 (1974).

Salpeter, E. E., and N. C. Wickramasinghe, Nature, 222, 442 (1969).

Serkowski, K., Adv. in Ast. and Ap. 1, 289 (1962).

Serkowski, K., and G. H. Reike, Ap. J. (Letters) 183, L103 (1973).

Shawl, S. J., Ph. D. dissertation, Univ. of Texas at Austin (1972).

Soifer, B. T., S. P. Willner, R. W. Russell, F. Puetter, K. M. Merrill, J. L. Pipher, J. R. Houck, W. J. Forrest, A. E. McCarthy, and F. C. Gillett

Spitzer, L., Diffuse Matter in Space, Interscience, New York (1968).

Stein, W. A., Ap. J. 144, 318 (1966).

Stein, W. A., and F. C. Gillett, Ap. J. (Letters) 155, L197 (1969).

Sterzer, F., D. Blattner, and S. Miniter, J. Opt. Soc. Am. 54, 62 (1964).

Treanor, P. J., Astronomical Techniques, W. A. Hiltner, ed., Univ. of Chicago Press, Chicago (1962).

Van de Hulst, H. C., Light Scattering by Small Particles, Wiley and Sons, N. Y. (1957).

Watson, W. D., Ap. J. 188, 35 (1974).

Woolf, N. J., Proc. IAU Symposium No. 52, Interstellar Dust and Related Topics, J. M. Greenberg and H. C. Van de Hulst, eds., Dordrecht:Reidel (1973).

Woolf, N. J., and E. P. Ney, Ap. J. (Letters) 155, L181 (1969).

Wynn-Williams, C. G., and E. E. Becklin, Pub. A.S.P. 86, 5 (1974).

Zaikowski, A., and R. F. Knacke, Ap. and Space Sci. 37, 3 (1975).

Zaikowski, A., R. F. Knacke, and C. C. Porco, Ap. and Space Sci. 35, 97 (1975).

Zuckerman, B., and P. Palmer, Ann. Rev. Ast. and Ap. 12, 297 (1974).